isvr Institute of Sound and Vibration Research

The Theory of a Continuous Damped Vibration Absorber to Reduce Broad-Band Wave Propagation in Beams

D.J. Thompson

ISVR Technical Memorandum No 968

January 2007

University of Southampton

SCIENTIFIC PUBLICATIONS BY THE ISVR

Technical Reports are published to promote timely dissemination of research results by ISVR personnel. This medium permits more detailed presentation than is usually acceptable for scientific journals. Responsibility for both the content and any opinions expressed rests entirely with the author(s).

Technical Memoranda are produced to enable the early or preliminary release of information by ISVR personnel where such release is deemed to the appropriate. Information contained in these memoranda may be incomplete, or form part of a continuing programme; this should be borne in mind when using or quoting from these documents.

Contract Reports are produced to record the results of scientific work carried out for sponsors, under contract. The ISVR treats these reports as confidential to sponsors and does not make them available for general circulation. Individual sponsors may, however, authorize subsequent release of the material.

UNIVERSITY OF SOUTHAMPTON

INSTITUTE OF SOUND AND VIBRATION RESEARCH

DYNAMICS GROUP

The theory of a continuous damped vibration absorber to reduce broad-band wave propagation in beams

by

D.J. Thompson

ISVR Technical Memorandum No: 968

January 2007

Authorised for issue by
Professor M.J. Brennan
Group Chairman

Acknowledgements

The analysis described here was carried out in part during a period of sabbatical leave in September 2005. The author is grateful to Trinity College, Cambridge for providing a visiting scholarship, to the Engineering Department of the University of Cambridge who hosted him during this period and to Dr Hugh Hunt in particular.

CONTENTS

Abstract

In order to attenuate structural waves in beams, a damped mass-spring absorber system is considered that is attached continuously along the beam length. Compared with other measures, such as impedance changes or tuned neutralisers applied at a single point, it is effective for excitation at any location along the beam. Although it is a tuned system, it can also be designed to be effective over a broad frequency range by the use of a high damping loss factor and multiple tuning frequencies. It has the advantage over constrained layer damping treatments that it can be effective even when the structural wavelength is long. The parameters controlling its behaviour are investigated and simple formulae developed, allowing optimisation of its performance. A particular application is the reduction of noise from a railway track, which requires the attenuation of structural waves along the rail to be increased typically in the frequency range 500 to 2000 Hz.

List of symbols

A	Cross-sectional area of beam
E	Young's modulus
I	Second moment of area of beam
L	Perimeter length of the beam cross-section
S	Surface area of beam
W_{rad}	Radiated sound power
c_0	Speed of sound in air
k	Wavenumber in the beam (real part)
k_0	Wavenumber of the unsupported beam at ω_0
k_a	Wavenumber of the unsupported beam at ω_a
k_b	Bending wavenumber in the unsupported beam
k_l	Longitudinal wavenumber in the unsupported beam
m_a'	Mass per unit length of absorber
m_b'	Mass per unit length of beam
m_s'	Mass per unit length of intermediate mass in two layer support
s	Stiffness of foundation per unit length
s_1	Stiffness of upper foundation layer per unit length
s_2	Stiffness of lower foundation layer per unit length
s_a	Stiffness of absorber per unit length
u	Longitudinal displacement of beam
v	Vibration velocity of beam
w	Bending displacement of beam
x	Distance along beam
Δ	Decay rate of wave in beam (dB/m)
β	Wavenumber in the beam (imaginary part)
$\delta\omega$	Frequency bandwidth of absorber
ε	Increment of frequency
η	Damping loss factor of foundation
η_1	Damping loss factor of upper foundation layer
η_2	Damping loss factor of lower foundation layer

η_a	Damping loss factor of absorber
η_b	Damping loss factor of beam
$\eta_{b,eq}$	Equivalent damping loss factor of beam due to absorber
μ	Ratio of absorber mass to beam mass
ρ_0	Density of air
σ	Radiation ratio of beam
ω	Angular frequency
ω_0	Cut-off frequency of beam on elastic foundation
ω_a	Tuning frequency of absorber
ω_b	Upper frequency of absorber stop band
ω_c	Mid frequency of absorber stop band
ζ	Damping ratio

1. Introduction

Structural wave propagation in beam structures can lead to unwanted noise transmission and radiation. The particular application providing the motivation for the present work is a railway track (Thompson *et al.* 2003, Jones *et al.* 2006) but many other examples exist, such as piping systems for fluids or gases (see e.g. Clark 1995, de Jong 1994), or beam-like components which are present in structures such as bridges, cranes and buildings. Such beam systems are often very long and may be characterised in the audio frequency range in terms of propagating waves rather than modal behaviour. Whereas geometrical attenuation plays a significant role in two- and three-dimensional structures, in a one-dimensional structure there is no attenuation with distance apart from the effect of damping or discontinuities. Thus, in lightly damped uniform beams, structural waves may propagate over large distances and noise may be transmitted far from its source, to be radiated as sound by the beam itself or by some receiver structure. To reduce the total noise radiated by a vibrating beam, the spatial attenuation must be increased.

The use of a damped mass-spring absorber system applied continuously on a beam is studied here. The purpose of introducing such a system is to attenuate structural waves over a broad frequency range, and for arbitrarily located excitation. A specific application of such a system to a railway track is discussed by Thompson *et al.* (2007) where, by sufficiently increasing the attenuation of vibration along the rail in a broad frequency band, the radiated noise from the track has been reduced by around 6 dB.

The focus in this report is on determining the effects of the various parameters controlling the behaviour of a continuous absorber attached to a beam and deriving simple formulae for this behaviour. After a discussion of the background to the problem, a simple model of a beam on an elastic foundation is first considered. The decay rates of waves in the beam and the effects of the support are illustrated. Using this as a basis, the analysis is extended to an unsupported beam to which a continuous absorber is attached, the absorber being treated as a frequency-dependent complex support stiffness. Approximate formulae are then derived for the effects of the absorber, illustrating simply the influence of mass and damping. The use of multiple tuning frequencies is also considered in order to widen the bandwidth of the absorber. It is then shown that the damping effect of an absorber system attached to a supported beam can be approximated by adding the separate spatial attenuations from the supported beam and the

beam with the absorber system. Finally some practical issues relating to the application of absorber systems to railway tracks are discussed.

2. Background

2.1 Techniques for reduction of vibration

Various vibration control techniques may be used in order to reduce such wave propagation in beams (Mead 2000).

Impedance changes at discontinuities, for example by added stiffness, mass, resilient connections or section changes, may be used to introduce reflection and thereby reduce transmitted power (Mead 2000, Cremer *et al.* 1988). In practice, such discontinuities cannot always be used, however. In the particular case of a railway track, continuous welded rail is used to avoid impact noise due to discontinuities in the rail running surface and it is therefore undesirable to reintroduce discontinuities.

To increase the damping, constrained layer or unconstrained layer damping treatments are particularly effective for relatively thin plate systems (Mead 2000, Nashif *et al.* 1985), but beams are often stiffer in order to carry structural loads. Consequently the structural wavelengths are long and surface strains are small so that, to be effective, the corresponding damping treatments would become too large for practical application. An absorber system responds to surface motion rather than strain and can therefore be arranged to be efficient at low frequencies (Zapfe & Lesieutre 1997).

2.2 Vibration absorbers

Mass-spring or mass-spring-damper systems are widely used to control the response of resonant structures, see Mead (2000), Nashif *et al.* (1985), Brennan & Ferguson (2004) and Hunt (1979). These are variously called tuned vibration absorbers, dynamic vibration absorbers, tuned mass dampers or vibration neutralisers. By appropriate choice of parameters, the frequency of an added mass-spring system can be matched to a resonance of the original structure or to a forcing frequency. The design of the system differs depending on whether the purpose is to suppress the response at a troublesome resonance frequency due to a broad-band excitation or to suppress the response at a troublesome forcing frequency. Following the

terminology used in (Brennan & Ferguson 2004) they may be called dynamic *absorbers* in the former case and vibration *neutralisers* in the latter case.

The performance in both situations increases as the added mass is increased. However, the need for damping in the added system depends on the application. In the case of a vibration absorber applied to deal with a resonance there is an optimum value of the damping; if it is too high the response is not modified at the original resonance, but if it is too low the response at modified resonances of the coupled system will remain a problem. In practice, relatively high values of damping loss factor are usually required for effective results (Brennan & Ferguson 2004). On the other hand, for neutralisers intended to suppress the response at some troublesome forcing frequency, the damping should be low to obtain good performance at the intended frequency. The low damping means that the bandwidth of operation becomes small. Therefore, in order to cover a broader frequency range, for example to allow for variations in the forcing frequency, either the damping has to be compromised or an adaptive system may be used (Brennan 1997a). Note that the term 'absorber' will be used throughout the remainder of this report, even when discussing undamped cases, as the practical applications envisaged have broad-band excitation and will generally require high damping.

The theory of the dynamic vibration absorber was first presented by Ormondroyd & den Hartog (1928). They demonstrated an application of an undamped cantilever beam on a generator bearing pedestal of a turbine to eliminate a problem at the turbine operating speed. Since then, dynamic absorbers have been applied in a wide variety of situations. In his book on the subject, Hunt (1979) discusses many examples of applications, including gas turbine blades, a footbridge, chimneys, suspended electricity cables, electric clippers, helicopters and multi-storey buildings.

Various practical designs exist and are discussed for example by Mead (2000), Nashif *et al.* (1985) and Hunt (1979). These include: cantilever with added mass, double cantilever with added masses, cruciform, pendulum, mass on elastomer in compression, mass on elastomer in shear and cylindrical shear type. It is also possible to use piezoelectric patches along with passive, resonant electronic circuits to form vibration absorbers (Maurini *et al.* 2004).

At its resonance frequency an undamped mass-spring system pins the host structure; it should therefore be tuned to the resonance of the original structure. However, to give the best effect

over a frequency band under random excitation, Den Hartog (1985) derived optimum values for the frequency of a damped absorber and its damping ratio in order to minimise the displacement response of the host structure, see also Mead (2000) and Brennan & Ferguson (2004). The absorber frequency should be tuned to $\omega = \omega_m / (1+\mu)$, where ω_m is the natural frequency of the original resonance to be damped and μ is the ratio of absorber mass to the (modal) mass of the host structure. The optimum damping ratio is found to be $\zeta = (3\mu / (8(1+\mu)^3))^{1/2}$.

Absorbers are generally intended to deal with a single resonance of the host structure and they therefore have only small effect at other structural resonances that lie far from the tuning frequency (Mead 2000). It is possible to add multiple absorbers on a structure tuned to deal with different resonances. Rana & Soong (1998) considered applying three absorbers to a three-degree-of-freedom building model to reduce the response to earthquake excitation, but they found that the addition of absorbers intended to deal with the second and third modes led to a slight increase in the response at the first mode due to the additional mass.

A recent high-profile vibration problem was the excessive lateral sway motion caused by crowds walking across the Millennium footbridge in London in June 2000 (Newland 2003, Newland 2004). This provided particular motivation for a renewed increase in research in this field. In an extensive review of this topic (Zivanovic *et al.* 2005), dynamic vibration absorbers are identified as a common solution for both lateral and vertical motion of footbridges. Other solutions include viscous dampers and the tuning of natural frequencies to avoid the main frequency region of excitation due to pedestrian-induced forces. The Millennium Bridge was subsequently modified to increase the damping ratios of lateral modes below 1.5 Hz from less than 1% to between 15% and 20% (Newland 2003). To achieve this the bridge was fitted with 37 viscous dampers acting between frames added beneath the deck and fours pairs of laterally acting vibration absorbers (Newland 2003, Zivanovic *et al.* 2005). Additionally, 26 pairs of vertically acting tuned absorbers were installed to increase the damping of vertical modes to between 5 and 10% (Newland 2003).

2.3 Application to waves in beams

Although most applications of absorber systems have been to resonant finite systems, lightly damped tuned neutralisers have also been considered for application at a point on a long beam such as a pipe to form an impedance change tuned to a particular forcing frequency (Clark

1995, Brennan 1998). This is seen as particularly effective at low frequencies. Due to the influence of near-field waves in the beam, the maximum blocking effect occurs at a frequency just above the tuning frequency of the mass-spring system if the system is arranged to apply a point force. At the tuning frequency itself only half of the incident energy in a bending wave is reflected, since the neutraliser effectively pins the beam. In (Clark 1995) the bandwidth of such a neutraliser, defined there as the frequency range over which the attenuation is greater than 3 dB, is found to be equal to $\omega_a \mu k/4$, where ω_a is the tuning frequency (the natural frequency of the grounded mass-spring system), k is the bending wavenumber in the beam and μ is the ratio of the mass of the neutraliser to the mass per unit length of the beam. Similarly, if the system applies a moment, the maximum effect occurs just below the tuning frequency (Clark 1995) and again only half the incident energy is reflected at the tuning frequency itself.

If it is required to attenuate structural wave propagation in the beam over a wide frequency range, such a mass-spring system applied at a single point is not suitable. Moreover, if the excitation can in principle be at any location along the beam, as is the case for a railway track, it is clear that some form of distributed treatment is required.

2.4 Distributed absorbers

Applications of absorbers distributed across a structure are much less common than those applied at a point intended to deal with particular modes of the structure.

Kashina & Tyutekin (1990) describe the use of a set of undamped resonators to reduce longitudinal or flexural waves in beams or plates. They envisage a group of mass-spring systems located over a certain length of the beam or plate and derive relations for the optimum mass and number of oscillators required to give attenuation over a specified frequency band.

Smith *et al.* (1986) give an analysis of a beam or plate with a continuous layer of absorbers applied to it. Their interest was in ship hulls. It was recognised that there is potential to use the mass of installed machinery in the ship as a distributed absorber with a high mass ratio. If mass is added that has no other function it must be much smaller but appreciable reductions may still be possible.

Analysis of an undamped absorber by (Smith *et al.* 1986) showed that waves in the beam (or plate) have a wavenumber with an imaginary part (i.e. strong decay) in the frequency range $1 < \omega / \omega_a < (1+\mu)^{1/2}$ where ω_a is the absorber tuning frequency and μ is the ratio of absorber mass to beam mass. It was recognised that adding damping to an array of absorbers on a plate or beam will reduce the wave attenuation at its peak value but spread the effect over a wider bandwidth. Numerical results were presented which showed this, but no analysis was given of the bandwidth or attenuation in the damped case. For the case considered by (Smith *et al.* 1986), it is stated that the undamped bandwidth is approximately correct if the damping loss factor is less than 0.1. Experiments were presented on an aluminium beam ending in a non-reflecting boundary which confirmed the predictions. It was also demonstrated experimentally that there is additional benefit if the absorber mass is distributed between two different tuning frequencies.

This work does not appear to have led to the development of distributed absorbers for attenuating structural waves. Other papers discussing distributed absorbers are generally concerned with the control of modes of vibration (Zapfe & Lesieutre 1997) or the control of acoustic transmission, for example in aerospace structures (Fuller *et al*. 1997, Marcotte *et al*. 1999, Estève & Johnson 2002).

2.5 Broadband absorbers

In order to broaden the bandwidth of an absorber, Hunt & Nissen (1982) describe the use of a particular practical form of non-linear softening spring. They show that the suppression bandwidth of a dynamic vibration absorber can be doubled using such a non-linear spring. An interesting concept that is widely considered is the development of a wideband vibration absorber by using an array of absorbers with a range of resonance frequencies (Brennan 1997b, Maidanik & Becker, 1999). For the same overall mass, the maximum impedance is reduced but the bandwidth is increased by a greater factor (Brennan 1997b). Strasberg & Feit (1996) present a simple deterministic derivation of the damping effect of a set of small oscillators attached to a large main structure, representing attached substructures. It is shown that the damping effect is primarily determined by the attached mass and not the damping of the attached systems.

3. Beam on elastic foundation

3.1 Undamped case

Before studying a continuous absorber attached to a beam, it is helpful to review the results for a beam on an elastic foundation. Consider a uniform Euler-Bernoulli beam with bending stiffness EI and mass per unit length m_b' on an elastic foundation of stiffness per unit length s, as shown in Figure 1. Initially damping is omitted.

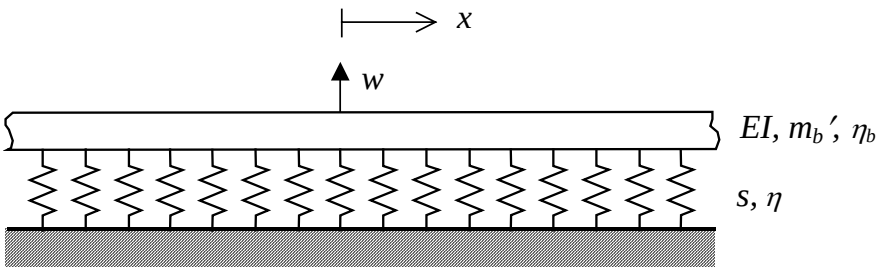

Figure 1. Beam on elastic foundation.

Considering harmonic motion at frequency ω, the free vibration satisfies (Graff 1991)

$$EI\frac{d^4w}{dx^4}+\left(s-m_b'\omega^2\right)w=0 \tag{1}$$

where w is the complex vibration amplitude and x is the coordinate along the beam direction. Seeking free wave solutions of the form $e^{-i\tilde{k}x}$, the wavenumber in the supported beam, $\tilde{k}=k-i\beta$, which may in principle be complex, satisfies

$$EI\,\tilde{k}^4+s-m_b'\omega^2=0 \tag{2}$$

which has solutions

$$\tilde{k}^2=\pm\sqrt{\frac{m_b'\omega^2-s}{EI}}=\pm k_b^2\sqrt{1-\frac{\omega_0^2}{\omega^2}} \tag{3}$$

where $\omega_0=(s/m_b')^{1/2}$ is the resonance frequency of the beam mass on the support stiffness and $k_b=(\omega^2 m_b'/EI)^{1/4}$ is the wavenumber of free waves in the unsupported beam. In the absence of damping, the wavenumber $\tilde{k}$ has purely real and imaginary solutions for frequencies above ω_0. These wavenumbers are always smaller in magnitude than the corresponding ones for the unsupported beam, but tend towards k_b at high frequency. At $\omega=\omega_0$, $\tilde{k}=0$ and the wavelength of free wave propagation becomes infinite, meaning that the whole beam moves

in phase along its length. This is referred to as the cut-off frequency for free waves in the supported beam (or sometimes 'cut-on' frequency).

For frequencies below ω_0, free wave propagation cannot occur. Instead, all waves have a wavenumber $\tilde{k}$ with a non-zero imaginary part β that is equal in magnitude to the real part, and waves occur in complex conjugate pairs. These waves are attenuated rapidly along the beam length. For $\omega << \omega_0$, the wavenumber in the fourth quadrant of the complex plane satisfies

$$k = -\beta \approx \frac{k_0}{\sqrt{2}} \tag{4}$$

where $k_0 = (s/EI)^{1/4}$, is the wavenumber of the unsupported beam at frequency ω_0.

The attenuation of a wave along the beam is determined by the imaginary part β and is zero for the propagating waves above ω_0 in the absence of damping. For a complex wavenumber $\tilde{k} = k - i\beta$, the amplitude reduces over a distance of 1 m by a factor $\exp(-\beta)$. The decay rate Δ may be expressed in dB/m and is given by

$$\Delta = 20 \log_{10}(\exp(\beta)) = 8.686\, \beta. \tag{5}$$

The rate of attenuation of vibration along the beam is important for the noise radiated. As shown in Appendix A, the total sound power radiated by a damped propagating wave in an infinite beam is inversely proportional to β and hence to the decay rate, Δ. Thus the sound power level (in dB) is actually related to $-10 \log_{10}(\Delta)$.

3.2 Effect of damping

Introducing damping into the support by means of a complex stiffness, $s \rightarrow s(1+\mathrm{i}\eta)$ and similarly for the beam $EI \rightarrow EI(1+\mathrm{i}\eta_b)$, gives complex wavenumbers

$$\tilde{k} = k_b (1 + i\eta_b)^{-1/4} \left(1 - \left(\frac{\omega_0}{\omega} \right)^2 (1 + i\eta) \right)^{1/4} \tag{6}$$

Three particular cases can be considered:

(i) At high frequency, for $\omega >> \omega_0$, the real part, $k \approx k_b$. The imaginary part is given by

$$\beta \approx k_b \left(\frac{\eta_b}{4} + \frac{\eta}{4} \left(\frac{\omega_0}{\omega} \right)^2 \right). \tag{7}$$

Since $k_b \propto \omega^{1/2}$, the first term is proportional to $\eta_b\omega^{1/2}$, whereas the second term is proportional to $\eta\omega^{-3/2}$. Thus, even if $\eta >> \eta_b$, at high enough frequency the effect of beam damping will predominate over that in the support.

(ii) At the cut-off frequency, $\omega = \omega_0$, support damping dominates and $k \approx \left(-i\eta s / EI\right)^{1/4}$. Of the various roots, the one with the smallest imaginary part (and hence the lowest attenuation) has $\tilde{k} = e^{-i\pi/8}\left(\eta s / EI\right)^{1/4}$. This gives,

$$k = 0.924\eta^{1/4}k_0, \ \beta = 0.383\eta^{1/4}k_0. \tag{8}$$

(iii) For $\omega << \omega_0$, the attenuation is large and the addition of damping has negligible effect compared with the undamped case. Therefore the wavenumber is given approximately by Eq. (4).

Figure 2 shows the wavenumber and wave decay rate in non-dimensional form for various values of damping loss factor. The frequency is shown relative to the cut-off frequency ω_0 whilst the real and imaginary parts of the wavenumber are non-dimensionalised by dividing by k_0, the wavenumber in the unsupported beam at ω_0.

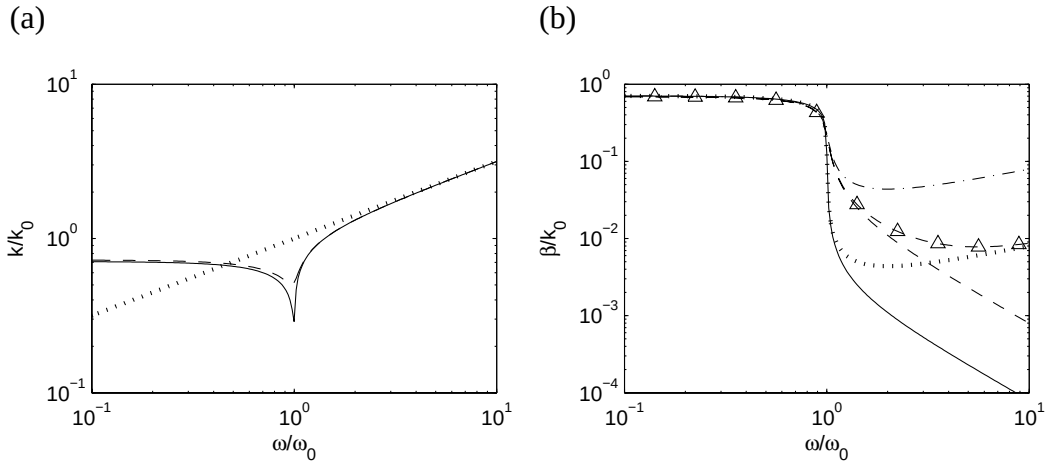

Figure 2. Wavenumbers of a beam on an elastic foundation. (a) Real part for $\eta_b = 0$: —, η = 0.01; – – –, $\eta = 0.1$, ·····, unsupported beam. (b) Imaginary part: —, $\eta = 0.01$, $\eta_b = 0$; – – –, $\eta = 0.1$, $\eta_b = 0$; ·····, $\eta = \eta_b = 0.01$; – Δ –, $\eta = 0.1$, $\eta_b = 0.01$; – · –, $\eta = \eta_b = 0.1$.

The real part of the wavenumber is affected by damping only in the vicinity of ω_0, where increasing the support damping η leads to an increase in the magnitude at the minimum. Results for different values of beam damping loss factor, η_b, are indistinguishable and

therefore not shown. Both real and imaginary parts of k/k_0 tend to $1/\sqrt{2}$ at low frequency, see Eq. (4). At high frequency the real part, k tends to k_b which is proportional to $\omega^{1/2}$. The high frequency behaviour of β can be seen to follow Eq. (7), with a slope of $\omega^{-3/2}$ in the absence of beam damping or $\omega^{1/2}$ where beam damping dominates. Extrapolating this high frequency behaviour back to $\omega = \omega_0$ gives $\beta/k_0 \rightarrow \eta/4$ or $\eta_b/4$ respectively. It can be seen that adding damping to the beam is effective over a much wider frequency range than adding damping to the support.

4. Beam with attached continuous absorber

Next, a beam is considered to which a continuous mass-spring system is attached, as shown in Figure 3. The beam is considered without any support stiffness in order to separate the effects of the absorber more readily; the combined effect will be considered in Section 7 below. The bending stiffness of the absorber mass is ignored as this will usually be much more flexible than the beam itself.

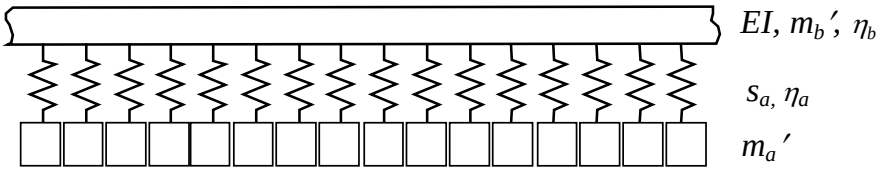

Figure 3. Beam connected to continuous mass-spring system.

4.1 Frequency-dependent stiffness

The absorber is assumed to have mass per unit length m_a' and stiffness per unit length s_a. These are related by the 'tuning frequency' of the absorber, $\omega_a = (s_a/m_a')^{1/2}$ which is the resonance frequency of the mass-spring system when attached to a rigid foundation. Hysteretic damping is added to the springs using a loss factor η_a. The analysis of Section 3 can be used directly by replacing s by a frequency-dependent 'support stiffness', $s(\omega)$ describing the attached mass-spring system, which is given by,

$$s(\omega) = \left(\frac{1}{s_a(1+i\eta_a)} - \frac{1}{\omega^2 m_a'} \right)^{-1} = \frac{\omega^2 s_a(1+i\eta_a)}{\omega^2 - \omega_a^2(1+i\eta_a)} \tag{9}$$

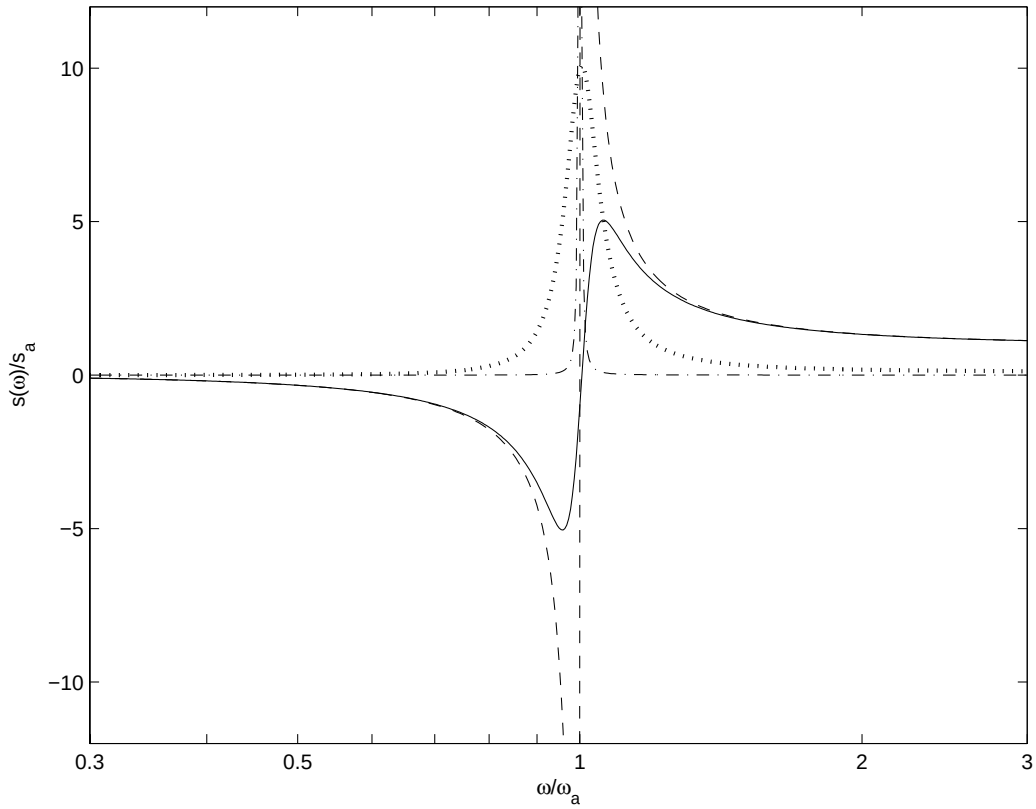

Figure 4. Equivalent stiffness $s(\omega)$ of tuned absorber normalised by s_a, for μ = 0.2. – – –, real part for η_a = 0.001; —, real part for η_a = 0.1; – · – ·, imaginary part for η_a = 0.001; ·····, imaginary part for η_a = 0.1.

The equivalent stiffness $s(\omega)$ from Eq. (9) is shown in non-dimensional form in Figure 4 for small and large damping values (η_a = 0.001 and 0.1). These are shown for a mass ratio μ of 0.2 where μ is defined as the ratio of the absorber mass to the beam mass, m_a' / m_b'. At high frequency the real part of $s(\omega)$ in Eq. (9) is positive (stiffness-like) as seen in the figure and $s(\omega)$ can be approximated by the damped absorber stiffness,

$$s(\omega) \to s_a(1 + i\eta_a) \text{ for } \omega >> \omega_a \tag{10}$$

Thus for $\omega >> \omega_a$, the beam can be expected to have similar behaviour to that described in Section 3. At ω_a, however, for an undamped system the denominator of Eq. (9) is zero giving $s(\omega) \to \infty$. For a damped system this becomes

$$s(\omega) \approx s_a\left(\frac{i}{\eta_a} - 1\right) \text{ for } \omega \approx \omega_a \tag{11}$$

The imaginary part of $s(\omega)$ is thus large in the vicinity of ω_a. Below ω_a, the real part of $s(\omega)$ is negative (mass-like), as seen in Figure 4. At low frequencies it is determined by the absorber mass, which becomes effectively rigidly connected to the beam. However, $s(\omega)$ also has a small imaginary part in this region which will prove to be important, so that it is useful to retain the second order terms to give

$$s(\omega) \approx -\omega^2 m_a' \left(1 + \frac{\omega^2}{\omega_a^{\,2}(1+i\eta_a)} \right) \text{ for } \omega << \omega_a \tag{12}$$

The wavenumber in the beam in the presence of the mass-spring system can be determined by substituting $s(\omega)$ from Eq. (9) into Eq. (2), to give

$$\tilde{k}^4 = k_b^4 \left(1 + \mu \frac{1+i\eta_a}{1+i\eta_a - (\omega^2/\omega_a^2)} \right) \tag{13}$$

4.2 Undamped absorber

Considering first an undamped absorber, below ω_a the wavenumber will be increased by the presence of the absorber, as $s(\omega)$ is mass-like. At low frequencies the effective mass of the beam becomes $m_b' + m_a'$ but as the frequency approaches ω_a the effective mass becomes large and the wavenumber increases towards infinity. Above the tuning frequency, $s(\omega)$ is stiffness-like, initially with a very large stiffness. Therefore a blocked region can be expected, where $\tilde{k}^2$ is imaginary, in the same way as for the beam on elastic foundation below its cut-off frequency.

For the undamped absorber, this blocked region will extend from ω_a to the cut-off frequency of free waves in the beam, ω_c, which is given by setting $\tilde{k}$ = 0 in Eq. (2), i.e.

$$s(\omega) - \omega^2 m_b' = \frac{\omega^2 s_a}{\omega^2 - \omega_a^2} - \omega^2 m_b' = 0 \tag{14}$$

This is satisfied by

$$\omega_c = \omega_a \sqrt{1+\mu} \approx \omega_a \left(1 + \frac{\mu}{2} \right) \quad \text{for } \mu << 1 \tag{15}$$

as found by Smith *et al.* (1986). The wavenumbers are shown in Figure 5 for various mass ratios. These have been normalised by the free beam wavenumber at ω_a, denoted $k_a = (\mu s_a/EI)^{1/4}$. In the blocked region, between ω_a and ω_c, the wavenumbers are large and in

conjugate pairs. For practical parameters, $\mu << 1$ and the undamped absorber has a fairly narrow blocked region.

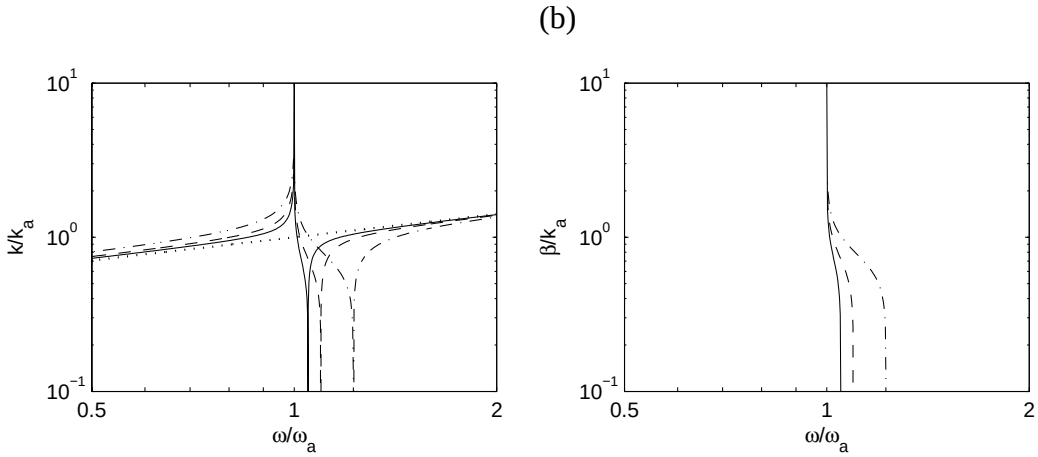

Figure 5. Wavenumbers of beam with undamped tuned absorber. —, μ = 0.1; – – –, μ = 0.2; – · – · μ = 0.5, ····· μ = 0. (a) Real part of first wave, (b) imaginary part of first wave.

In the absence of damping, non-zero spatial attenuation only occurs in the blocked region; elsewhere $\tilde{k}$ is real. At ω_a the decay rates tend to infinity, while at ω_c they tend to 0, as seen in Figure 5(b). Between these extremes the mass ratio affects the width of the blocked region but not the magnitude of the decay rates within this region.

This can also be shown analytically by considering the frequency ω_b given by $\omega_b^{\,2} = \omega_a^{\,2}(1+\mu/2)$ which is roughly in the centre of the blocked region. Substituting this into Eq. (9) gives

$$s(\omega_b) = \frac{\omega_b^{\,2} m_a'(1+i\eta_a)}{\mu/2 - i\eta_a} \tag{16}$$

which in the undamped case reduces to

$$s(\omega_b) = 2\omega_b^{\,2} m_b' \tag{17}$$

Hence, the wavenumber at ω_b is given by

$$\tilde{k} = k_b(-1)^{1/4} = k_b \frac{1-i}{\sqrt{2}} \tag{18}$$

which is independent of μ for $\mu << 1$. It increases slightly if μ is large, as k_b will be slightly higher at ω_b than at ω_a.

4.3 Damped absorber

By adding damping to the mass-spring system, the frequency range in which beam vibration is attenuated can be increased. Results obtained for different damping loss factors are shown in Figures 6 to 8 for an absorber mass of $\mu = 0.1$, 0.2 and 0.5. The imaginary part of the wavenumber is related to the decay rate according to Eq. (5). It is again shown normalised by the free beam wavenumber at ω_a.

Clearly, as the damping is increased, particularly for large values, the decay rate at the peak is reduced whilst the height of the flanks is increased. Comparing the different figures, it can be seen that, as the mass ratio is increased, the blocked region becomes wider, as was seen in Figure 5 for the undamped case, and the decay rate at the flanks is increased. These effects will be demonstrated analytically in Section 5.

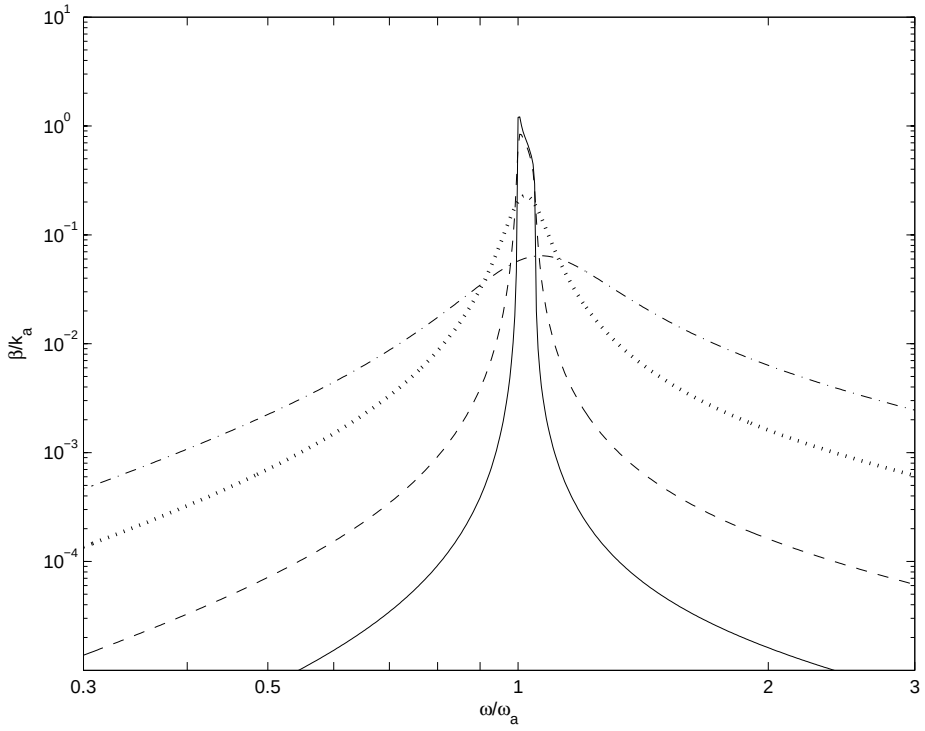

Figure 6. Normalised decay rate of beam with tuned absorber, $\mu = 0.1$. —, $\eta_a = 0.001$; – – –, $\eta_a = 0.01$; ·····, $\eta_a = 0.1$; – · – ·, $\eta_a = 0.4$.

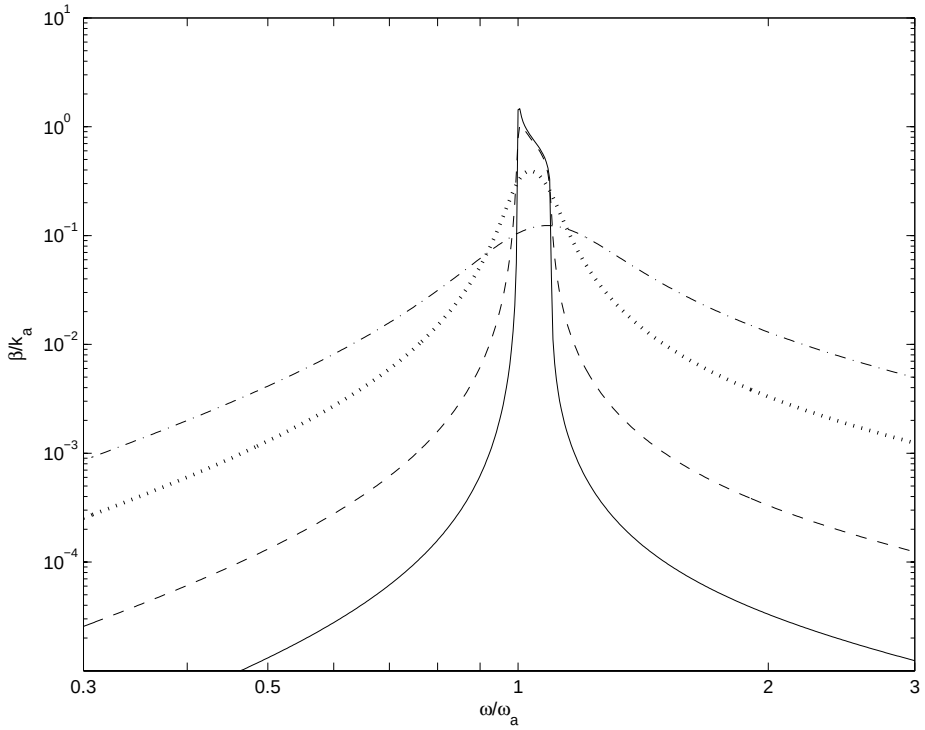

Figure 7. Normalised decay rate of beam with tuned absorber, $\mu = 0.2$. —, $\eta_a = 0.001$; – – –, $\eta_a = 0.01$; ·····, $\eta_a = 0.1$; – · – ·, $\eta_a = 0.4$.

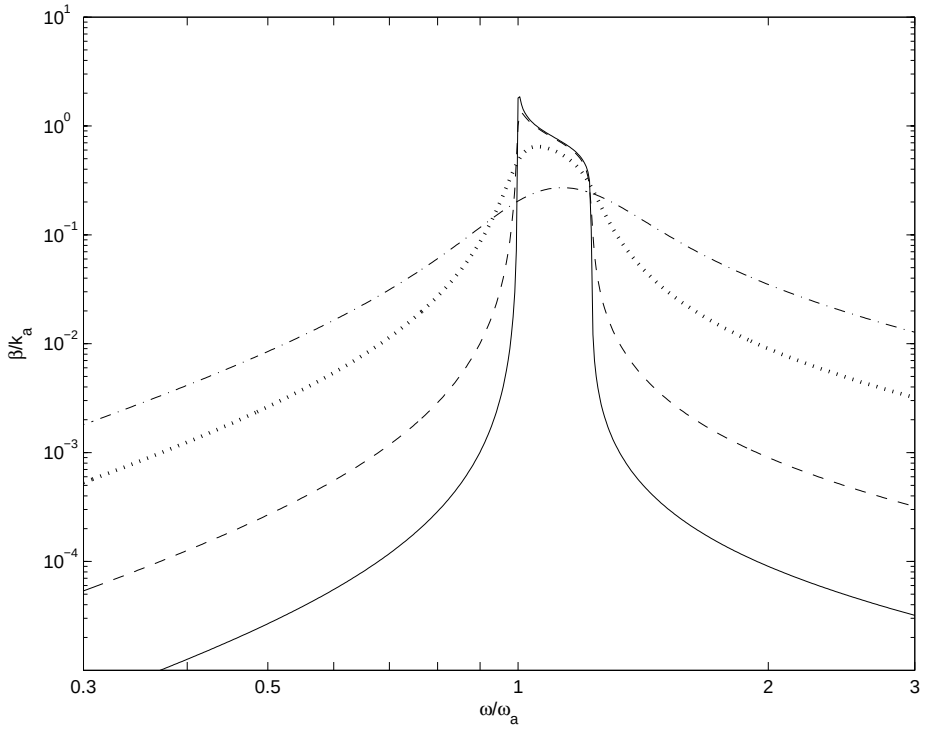

Figure 8. Normalised decay rate of beam with tuned absorber, $\mu = 0.5$. —, $\eta_a = 0.001$; – – –, $\eta_a = 0.01$; ·····, $\eta_a = 0.1$; – · – ·, $\eta_a = 0.4$.

4.4 Motion of absorber mass

The vibration of the absorber mass, w_a is given by

$$\tau = \frac{w_a}{w} = \frac{s_a(1+i\eta_a)}{s_a(1+i\eta_a) - \omega^2 m_s'} = \frac{(1+i\eta_a)}{(1+i\eta_a) - \frac{\omega^2}{\omega_a{}^2}} \tag{19}$$

This is shown in Figure 9 for different values of damping. The result is independent of absorber mass once the frequency is normalised by ω_a. This is the conventional transmissibility of a single degree of freedom system. At low frequencies $\tau \to 1$, while at high frequencies $\tau \to -\omega_a{}^2 / \omega^2$. Close to ω_a the absorber mass has large motion for low damping. For a loss factor of 0.4 it has an amplitude of motion at most a factor of 2.7 greater than that of the beam.

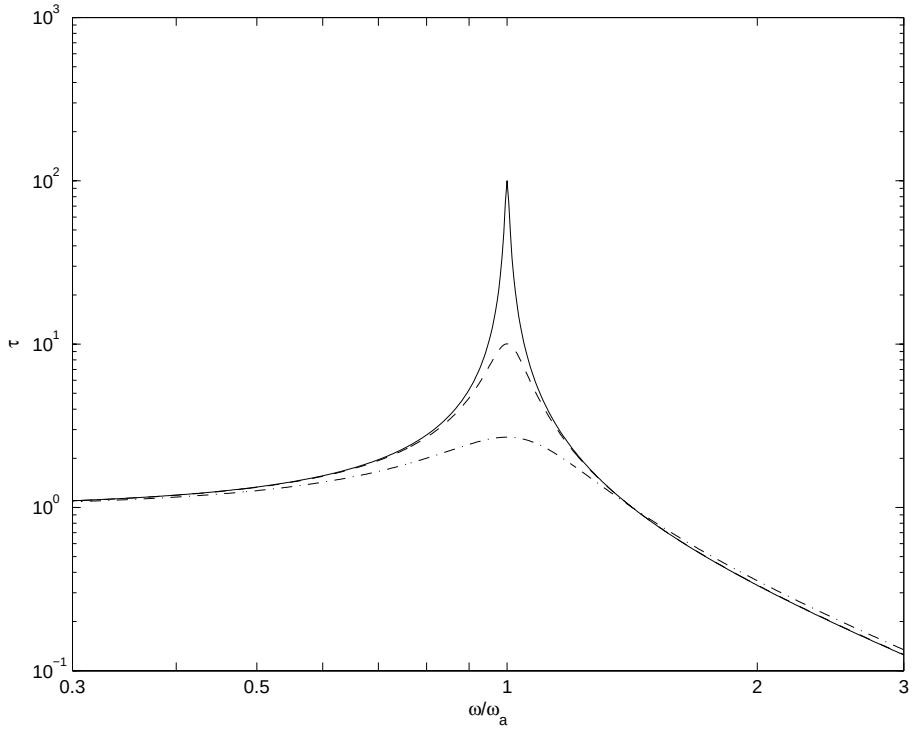

Figure 9. Ratio of absorber mass displacement to beam displacement (modulus). —, η_a = 0.01; – – –, η_a = 0.1; – · – ·, η_a = 0.4.

This motion of the absorber mass may lead to additional noise radiation. However, if $\mu << 1$ the absorber mass is likely to be small in size compared with the beam and consequently its noise radiation should also be lower. For example, for compact masses of the same density as the beam, the cross-sectional areas would be approximately in the ratio μ. The radius a of the

equivalent cylinders will therefore be approximately in the ratio $\mu^{1/2}$. At low frequencies where $ka << 1$, with k the acoustic wavenumber, the radiation ratio of a long oscillating cylinder is proportional to $(ka)^3$ (Fahy 1985), which will be in the ratio $\mu^{3/2}$. Thus the power radiated by a given vibration amplitude of the masses will be a factor μ^2 times that of the beam. As the power is proportional to the square of the velocity, the overall effect is $(\mu\tau)^2$. For example with $\eta_a = 0.4$ and $\mu = 0.2$, the sound power from the absorber mass is at most a factor of 0.54 times that of the beam, the presence of the absorber mass leading to an increase of 2 dB. However, this occurs at the frequency where the attenuation of bending waves is greatest, so the effect on broad-band noise is much less than this and may be neglected. For lower values of damping or for masses which are not compact the noise from the absorbers may be significant.

5. Approximate formulae

5.1 Approximate formulae for the decay rate far from the tuning frequency

The effects shown in Figures 6 to 8 can be demonstrated analytically. First the decay rate far from the tuning frequency is considered. From Eq. (3) the imaginary part of the wavenumber is given by

$$\beta = -k_b \,\mathrm{Im}\left\{\left(1 - \frac{s(\omega)}{m_r'\omega^2}\right)^{1/4}\right\} \tag{20}$$

At high frequencies, from Eq. (10) and substituting $s_a = m_a'\omega_a^2$,

$$\beta \approx \frac{k_b}{4}\frac{\omega_a^{\,2}}{\omega^2}\mu\eta_a \quad \text{for } \omega >> \omega_a \tag{21}$$

Similarly at low frequencies, from Eq. (12)

$$\beta \approx \frac{k_b}{4}\frac{\omega^2}{\omega_a^{\,2}}\frac{\mu\eta_a}{(1+\mu)^{3/4}(1+\eta_a^{\,2})} \quad \text{for } \omega << \omega_a \tag{22}$$

which for small values of μ and η_a reduces to

$$\beta \approx \frac{k_b}{4}\frac{\omega^2}{\omega_a^{\,2}}\mu\eta_a \quad \text{for } \omega << \omega_a \tag{23}$$

Comparing Eq. (21) and (23), these both increase directly in proportion to the mass ratio μ and the damping loss factor η_a. This is confirmed by reference to the results in Figures 6 to 8 for low and high frequencies.

The frequency dependence is complicated by the presence of k_b which is proportional to $\omega^{1/2}$ so that below the tuning frequency β is proportional to $\omega^{5/2}$ while at high frequency it decreases with $\omega^{-3/2}$. It is possible to simplify the interpretation by considering an equivalent loss factor of the beam which will be defined by (compare Eq. (7))

$$\eta_{b,eq} = \frac{4\beta}{k_b} \tag{24}$$

Thus

$$\eta_{b,eq} \approx \frac{\omega^2}{\omega_a{}^2} \mu\eta_a \quad \text{for } \omega << \omega_a \tag{25}$$

$$\eta_{b,eq} \approx \frac{\omega_a{}^2}{\omega^2} \mu\eta_a \quad \text{for } \omega >> \omega_a \tag{26}$$

These results only apply at very low levels of decay rate and cannot be used to determine a useful frequency 'bandwidth' of the absorber effect. In Figures 6 to 8 it can be seen that the straight parts of the graphs only occur well below $\omega_a/2$ and above $2\omega_a$. The curved flanks will be considered further below.

5.2 Approximate formulae for the decay rate in the blocked zone

In this section the decay rate at the peak will be determined. In order to estimate this, it is convenient to consider the frequency ω_b given in Section 4.2 above, which is at the centre of the blocked zone for the undamped case. Evaluating the imaginary part of the wavenumber at this frequency from Eq. (20),

$$\beta = -k_b \,\mathrm{Im}\left\{\left(1 - \frac{\mu(1+i\eta_a)}{\mu/2 - i\eta_a}\right)^{1/4}\right\} \text{ for } \omega = \omega_b \tag{27}$$

Two extreme cases can be considered. Firstly, for small damping $\eta_a << \mu/2$ (and $\eta_a << 1$)

$$\beta \approx -k_b \,\mathrm{Im}\left\{\left(-1 - 2i\eta_a - 2i\frac{\eta_a}{\mu}\right)^{1/4}\right\} \tag{28}$$

Here the imaginary terms inside the brackets are small compared with –1, so that the decay rate is given by the earlier result for the undamped case, see Eq. (18), which is independent of both the mass ratio and the loss factor,

$$\beta = \frac{1}{\sqrt{2}} k_b \tag{29}$$

The 'equivalent loss factor' of the beam is $\eta_{b,eq} \approx 2\sqrt{2} = 2.83$.

Secondly, for large damping $\eta_a >> \mu/2$ (and $\mu << 2$), Eq. (27) reduces to

$$\beta = \frac{k_b}{4}\frac{\mu}{\eta_a} \tag{30}$$

This increases as the mass ratio increases but *reduces* as the damping of the absorber increases. The equivalent loss factor of the beam is

$$\eta_{b,eq} = \frac{\mu}{\eta_a} \tag{31}$$

Reference to Figures 6 to 8 confirms that the damping effect in the blocked region is independent of η_a at low values and reduces as η_a increases according to Eq. (30). Comparing the results for different mass ratios, the width of the blocked region increases with increasing μ, and for high values of η_a its height is increased as μ increases.

5.3 Bandwidth of absorber

It is desriable to determine the bandwidth of the absorber, that is, the frequency bandwidth for which the decay rate (or equivalent loss factor) is above a certain value. It has been noted that Eqs (21, 23) cannot be used practically for this purpose as they describe the behaviour too far from the blocked region. Consider instead frequencies in the vicinity of ω_a and write $\omega = \omega_a(1+\varepsilon)$. Then provided that $|\varepsilon| << 1$, from Eq. (13)

$$\frac{\eta_{b,eq}}{4} = \frac{\beta}{k_b} \approx -\mathrm{Im}\left\{\left(1+\mu\frac{(1+i\eta_a)}{i\eta_a - 2\varepsilon}\right)^{1/4}\right\} \tag{32}$$

Expanding

$$\frac{\eta_{b,eq}}{4} \approx -\mathrm{Im}\left\{\left(\frac{1+\left(\frac{2\varepsilon}{\eta_a}\right)^2 + \mu - \frac{2\varepsilon\mu}{\eta_a{}^2} - \frac{i\mu}{\eta_a}(1+2\varepsilon)}{1+\left(\frac{2\varepsilon}{\eta_a}\right)^2}\right)^{1/4}\right\} \tag{33}$$

Provided that $\eta_{b,eq} << 4$, the imaginary part of the expression inside the round brackets will be small compared with the real part, allowing it to be expressed as

$$\frac{\eta_{b,eq}}{4} \approx \left(\frac{1+\left(\frac{2\varepsilon}{\eta_a}\right)^2 + \mu - \frac{2\varepsilon\mu}{\eta_a{}^2}}{1+\left(\frac{2\varepsilon}{\eta_a}\right)^2} \right)^{1/4} \frac{1}{4} \left(\frac{\frac{\mu}{\eta_a}(1+2\varepsilon)}{1+\left(\frac{2\varepsilon}{\eta_a}\right)^2 + \mu - \frac{2\varepsilon\mu}{\eta_a{}^2}} \right) \tag{34}$$

Consistent with the assumption that Re($\tilde{k}$) ≈ k_b ≈ k_a, the first expression in Eq. (34), which is equal to the real part associated with Eq. (34), is approximately equal to 1 and can be neglected. The remaining expression can be solved for ε:

$$\eta_{b,eq}\left(1+\left(\frac{2\varepsilon}{\eta_a}\right)^2 + \mu - \frac{2\varepsilon\mu}{\eta_a{}^2}\right) \approx \frac{\mu}{\eta_a}(1+2\varepsilon) \tag{35}$$

giving

$$(2\varepsilon) = \frac{\mu}{2}\left(1+\frac{\eta_a}{\eta_{b,eq}}\right) \pm \sqrt{\left(\frac{\mu}{2}\left(1+\frac{\eta_a}{\eta_{b,eq}}\right)\right)^2 + \frac{\eta_a\mu}{\eta_{b,eq}} - \eta_a{}^2(1+\mu)} \tag{36}$$

This has two roots ε_+ and ε_- which are above and below zero (either side of ω_a) so that the bandwidth $\delta\omega$ within which $\eta_{b,eq}$ is greater than a certain value is given by

$$\frac{\delta\omega}{\omega_a} = \varepsilon_+ - \varepsilon_- = \sqrt{\left(\frac{\mu}{2}\left(1+\frac{\eta_a}{\eta_{b,eq}}\right)\right)^2 + \frac{\eta_a\mu}{\eta_{b,eq}} - \eta_a{}^2(1+\mu)} \tag{37}$$

For the limiting case of low damping, $\eta_a \to 0$, this reduces to $\mu/2$, which agrees with Eq. (15). When η_a is not small and $\mu << 1$, the bandwidth in Eq. (37) can be approximated by

$$\frac{\delta\omega}{\omega_a} \approx \sqrt{\frac{\eta_a\mu}{\eta_{b,eq}} - \eta_a{}^2} \tag{38}$$

Figure 10 shows the actual bandwidth obtained for μ = 0.1 for various levels of damping, determined numerically from results such as those in Figure 6. Each plot shows the bandwidth at a particular value of equivalent loss factor. Also shown are the estimates obtained from Eq. (37). These can be seen to agree very well with the observed bandwidths in most cases. Figure 11 shows corresponding results for μ = 0.5. Agreement is found to be slightly less good for this case, as the approximations made are no longer valid when ε is not small. Also shown in Figures 10 and 11 are the estimates obtained using the approximate expressions according to Eqs (15) and (38). It can be seen that these give good agreement at low and high values of η_a respectively.

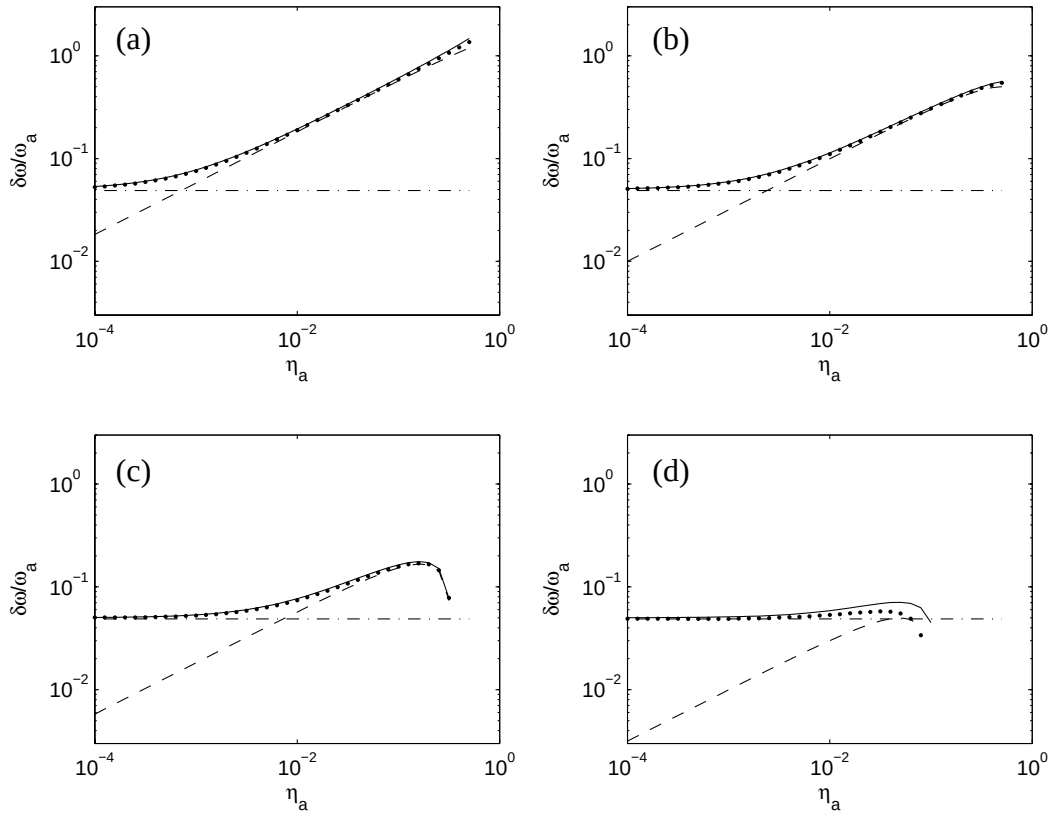

Figure 10. Relative frequency bandwidth at various levels of equivalent loss factor, $\mu = 0.1$. (a) $\eta_{b,eq} = 0.03$, (b) $\eta_{b,eq} = 0.1$, (c) $\eta_{b,eq} = 0.3$, (d) $\eta_{b,eq} = 1$. ●●●●●, from decay rate curves; —, full estimate, Eq. (37); – – –, simplified estimate from Eq. (38); – · – · estimate from undamped system, Eq. (15).

The bandwidth according to Eq. (38) is dominated by the first term except for very high values of η_a where the peak of the decay rate curve is approached. From Eq. (31) it will be recalled that for high damping the peak is characterised by $\eta_{b,eq} = \mu/\eta_a$, which gives $\delta\omega = 0$ in Eq. (38). However, for most of the range of values considered and where $\eta_a > 0.01$, a reasonable estimate is given by

$$\frac{\delta\omega}{\omega_a} \approx \sqrt{\frac{\eta_a \mu}{\eta_{b,eq}}} \tag{39}$$

This shows directly the benefit of increasing the absorber damping and mass ratio on the bandwidth. However, as has been seen, the effect is limited by the second term in Eq. (38) if the absorber loss factor is increased too far.

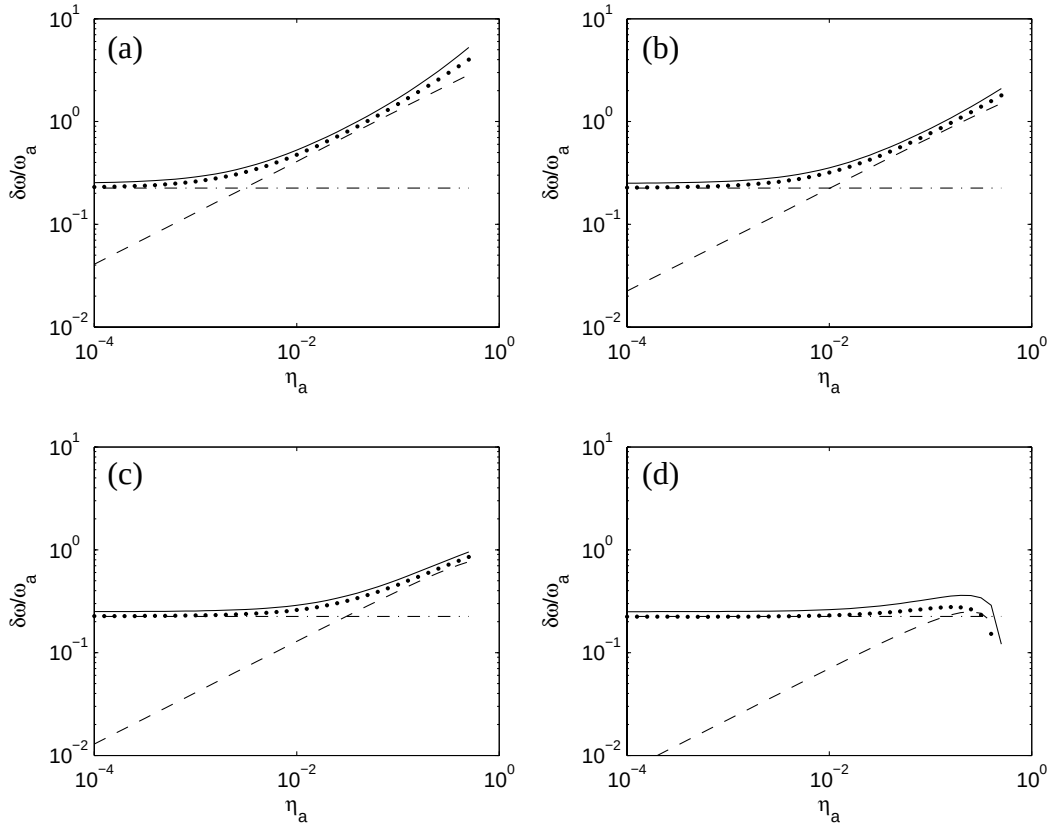

Figure 11. Relative frequency bandwidth at various levels of equivalent loss factor, $\mu = 0.5$. (a) $\eta_{b,eq} = 0.03$, (b) $\eta_{b,eq} = 0.1$, (c) $\eta_{b,eq} = 0.3$, (d) $\eta_{b,eq} = 1$. ●●●●●, from decay rate curves; —, full estimate, Eq. (37); – – –, simplified estimate from Eq. (38); – · – · estimate from undamped system, Eq. (15).

It may be noted from these results that the bandwidth of the absorber is independent of the beam wavenumber, see Eq. (38). Thus by selecting an appropriate tuning frequency, such an absorber can be used to treat any frequency. In particular, it can be effective even at low frequencies where the wavelength in the beam is too long for constrained layer damping treatments to be used successfully.

6. Multiple tuning frequencies

It is worthwhile considering the potential benefit of dividing the absorber mass between two or more added systems tuned to different frequencies such that their bandwidths do not overlap (but are adjacent to each other). Such an approach has been used for discrete neutralisers, for example by Brennan (1997b), see also Maidanik and Becker (1999).

For a continuous system, the combined bandwidth of two such absorbers is then

$$\delta\omega \approx \omega_{a,1}\sqrt{\frac{\mu_1\eta_{a,1}}{\eta_{b,eq}}} + \omega_{a,2}\sqrt{\frac{\mu_2\eta_{a,2}}{\eta_{b,eq}}} \tag{40}$$

Assuming that the mass is equally divided, $\mu_1 = \mu_2 = \mu/2$, and that the loss factors are identical,

$$\delta\omega \approx \left(\frac{\omega_{a,1} + \omega_{a,2}}{\sqrt{2}}\right)\sqrt{\frac{\mu\eta_a}{\eta_{b,eq}}} \tag{41}$$

This gives a bandwidth that is wider than for a single absorber of the same overall mass by a factor of approximately $\sqrt{2} = 1.41$ provided that the first term in Eq. (38) remains dominant. Similarly, dividing the mass equally between three absorbers of different frequencies leads to a bandwidth which is $\sqrt{3} = 1.73$ wider than the single absorber, etc. However, as the mass is divided further, the height of each damping peak is reduced so that it becomes more difficult to obtain high decay rates. Thus there is a trade-off between bandwidth and high decay rate.

Figure 12 shows results calculated for single, double and triple absorbers with a loss factor of 0.4 and the same combined mass of $\mu = 0.2$. Also shown is a result for ten absorbers with the same combined mass. The tuning frequencies have been chosen in each case to ensure that the equivalent loss factor $\eta_{b,eq}$ just remains above 0.1 in a continuous frequency band. Although the bandwidth is clearly increased, it can be seen that the height of the peaks is reduced. The net effect for a broad-band excitation can be found by integrating the curves in Figure 12 and is only the equivalent of 1.2 dB greater for ten absorbers than for one, although the actual benefit will depend on the form of the excitation spectrum. The result for ten absorbers can be seen to be close to a limiting case such that, if the mass is further subdivided while maintaining the same beam loss factor, no further gain is obtained.

The peaks can be observed to increase slightly in height with increasing frequency, due to the influence of $k_b \propto \omega^{1/2}$. This suggests that if the target is for a particular value of decay rate, it would be more efficient to divide the mass unevenly between the various tuning frequencies, with more mass concentrated at the lower frequencies.

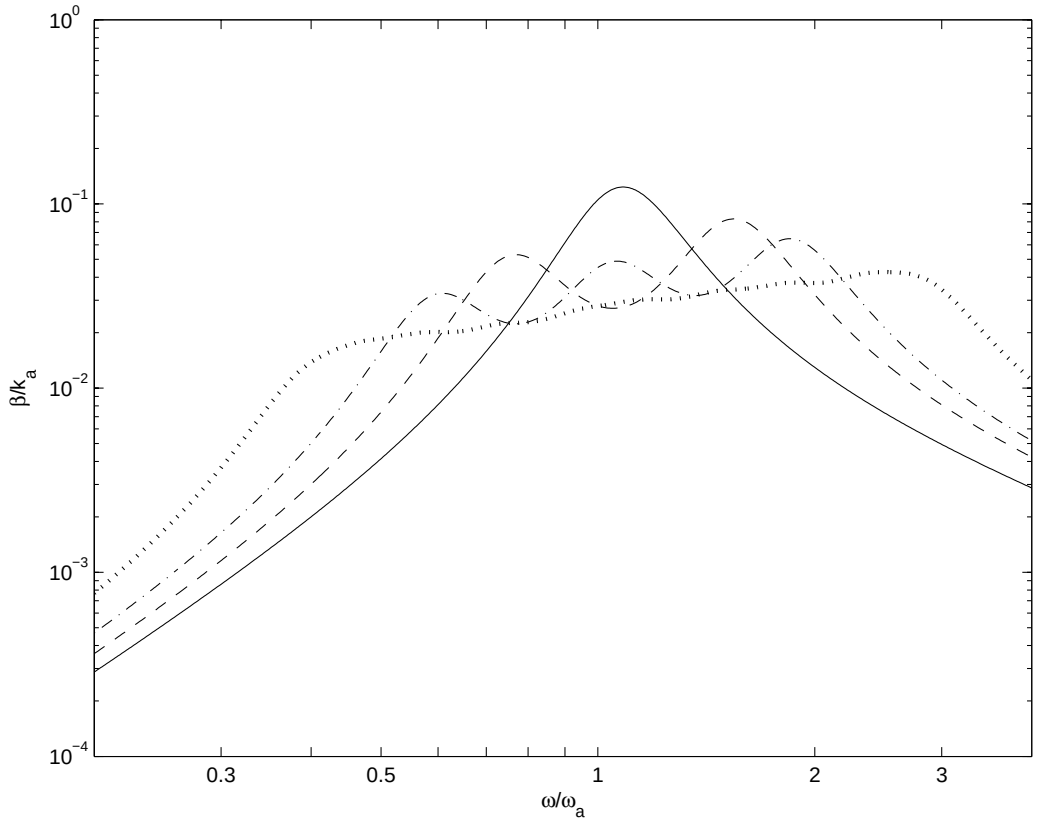

Figure 12. Decay rate of beam with tuned absorbers, η_a = 0.4. —, single absorber with μ = 0.2 tuned to ω_a; – – –, two absorbers each with μ_i = 0.1 tuned to 0.72ω_a and 1.45ω_a; – · – · three absorbers each with μ_i = 0.067, tuned to 0.57ω_a, ω_a and 1.75ω_a; ····· ten absorbers each with μ_i = 0.02, tuned to frequencies between 0.38ω_a and 2.7ω_a.

7. Absorber applied to beam on elastic foundation

If an absorber system is applied to a beam on an elastic foundation, the dynamic behaviour should be predicted using both the foundation stiffness and the equivalent stiffness of the absorber in Eq. (9) to give the total frequency-dependent stiffness $s(\omega)$. However, since the absorber is designed to increase the attenuation of propagating waves in the region above the cut-off frequency due to the support, it is reasonable to assume that $\omega_0 << \omega_a$. Where these frequencies are well separated, it is possible to predict the vibration decay rate as the sum of that of the supported beam with no absorber and of the free beam with absorber. Such an approach was used by (Thompson *et al.* 2007) in determining the decay rates of a rail

absorber, in order to simplify the analysis. In this section, the validity of this approach is investigated.

Including the foundation stiffness s_1 into Eq. (9), gives (in the absence of damping)

$$s(\omega) = s_1 + \frac{\omega^2 s_a}{\omega^2 - \omega_a^2} \tag{42}$$

This yields a cut-off frequency, satisfying $m_r'\omega^2 - s(\omega) = 0$, which for $\omega << \omega_a$ gives

$$\omega_0' \approx \sqrt{\frac{s_1}{m_b'+m_a'}} = \frac{\omega_0}{\sqrt{1+\mu}} \tag{43}$$

This is lower than that in the absence of the absorber, due to the addition of the absorber mass. Waves are blocked below ω_0'.

Including damping in each of the springs and the beam itself, the imaginary part of the wavenumber is given by a modified form of Eq. (20),

$$\beta = -\mathrm{Im}\left\{ k_b\left(1+i\eta_b\right)^{-1/4}\left(1-\frac{\omega_0^2}{\omega^2}(1+i\eta) - \frac{\mu(1+i\eta_a)}{(\omega^2/\omega_a^2)-(1+i\eta_a)}\right)^{1/4}\right\} \tag{44}$$

Around and above ω_a the final term dominates. This is related to the absorber, and the decay rate can be estimated using the relations in Section 4. For $\omega >> \omega_a$,

$$\beta \approx k_b\left(\frac{\eta_b}{4} + \frac{\eta\omega_0^2}{4\omega^2} + \frac{\eta_a\mu\omega_a^2}{4\omega^2}\right) \tag{45}$$

The first two terms represent the damping effect of the beam and foundation layer respectively, given by Eq. (7) and the third term is that of absorber above its tuning frequency, Eq. (21). This shows that the damping effects can be simply combined by adding the separate decay rates.

For frequencies well below ω_a, Eq. (44) may be approximated as

$$\beta \approx -k_b\,\mathrm{Im}\left\{\left(1+i\eta_b\right)^{-1/4}\left(1-\frac{\omega_0^2}{\omega^2}(1+i\eta)+\mu\right)^{1/4}\right\} \tag{46}$$

This can be expressed as

$$\beta \approx -k_b\left(1+\mu\right)^{1/4}\,\mathrm{Im}\left\{\left(1+i\eta_b\right)^{-1/4}\left(1-\frac{\omega_0^2}{\omega^2}\frac{(1+i\eta)}{(1+\mu)}\right)^{1/4}\right\} \tag{47}$$

which is equivalent to the result in Eq. (7) for a beam of mass $m_b'(1+\mu)$ on the elastic foundation. Thus the absorber actually reduces the attenuation in this region, due to the increase in mass and the corresponding shift in cut-off frequency ω_0'.

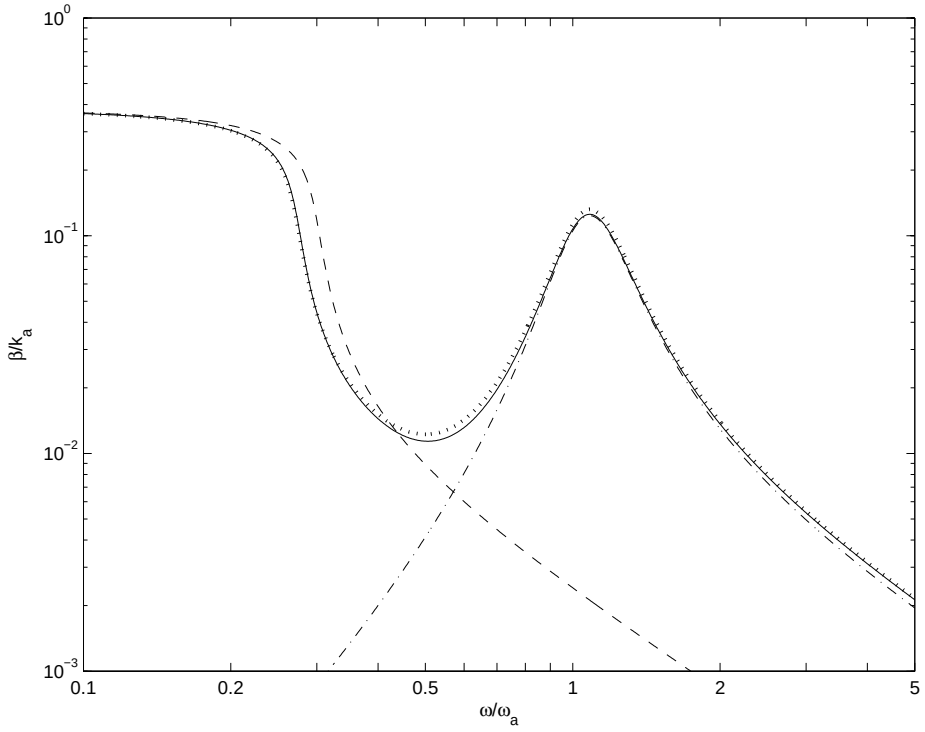

Figure 13. Normalised decay rate of supported Euler-Bernoulli beam with tuned absorbers, $\mu = 0.2$, $\omega_0 = 0.3\omega_a$, $\eta = 0.1$, $\eta_a = 0.4$. ·····, direct calculation of supported beam with absorber; – · – ·, absorber on free beam; – – –, supported beam with no absorber; —, sum of decay rates of absorber on free beam and supported beam including absorber mass.

Figure 13 shows the normalised decay rate in the form of β/k_a for the beam on elastic foundation with absorber, according to Eq. (44). The initial cut-off frequency for the beam on elastic foundation ω_0 is here set to $0.3\omega_a$. For simplicity the beam damping loss factor η is set to zero. In addition, the separate results are shown for the beam on elastic foundation and the unsupported beam with absorber. As noted above, the effective cut-off frequency due to the support stiffness is reduced, here by about 9%, and consequently the decay rate is reduced slightly between about $0.2\omega_a$ and $0.5\omega_a$ (around and above ω_0) by the addition of the absorber mass. By adjusting the mass of the beam to include that of the absorber, a good approximation to the exact result can be obtained using the sum of the two separate results.

Figure 14 shows corresponding results for $\mu = 0.5$. The shift in cut-off frequency is greater for the larger mass ratio; in this case it is 18%. Again the sum of the two separate results gives a good approximation to the actual result when the absorber mass is added to the supported beam.

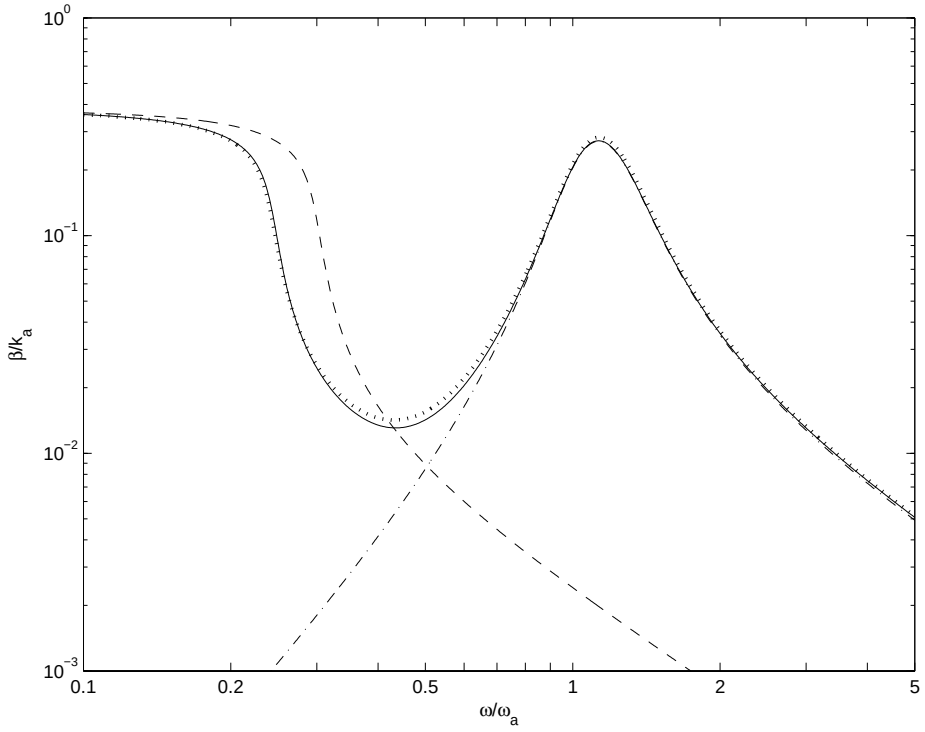

Figure 14. Normalised decay rate of supported Euler-Bernoulli beam with tuned absorbers, $\mu = 0.5$, $\omega_0 = 0.3\omega_a$, $\eta = 0.1$, $\eta_a = 0.4$. ·····, direct calculation of supported beam with absorber; – · – ·, absorber on free beam; – – –, supported beam with no absorber; —, sum of decay rates of absorber on free beam and supported beam including absorber mass.

In Figure 15 results are shown for a stiffer support, giving $\omega_0 = 0.5\omega_a$, with $\mu = 0.2$. Here, in the vicinity of ω_a the combined effect is slightly larger than predicted by adding the separate effects. However, the difference is still less than 1 dB and the approximate approach is acceptable.

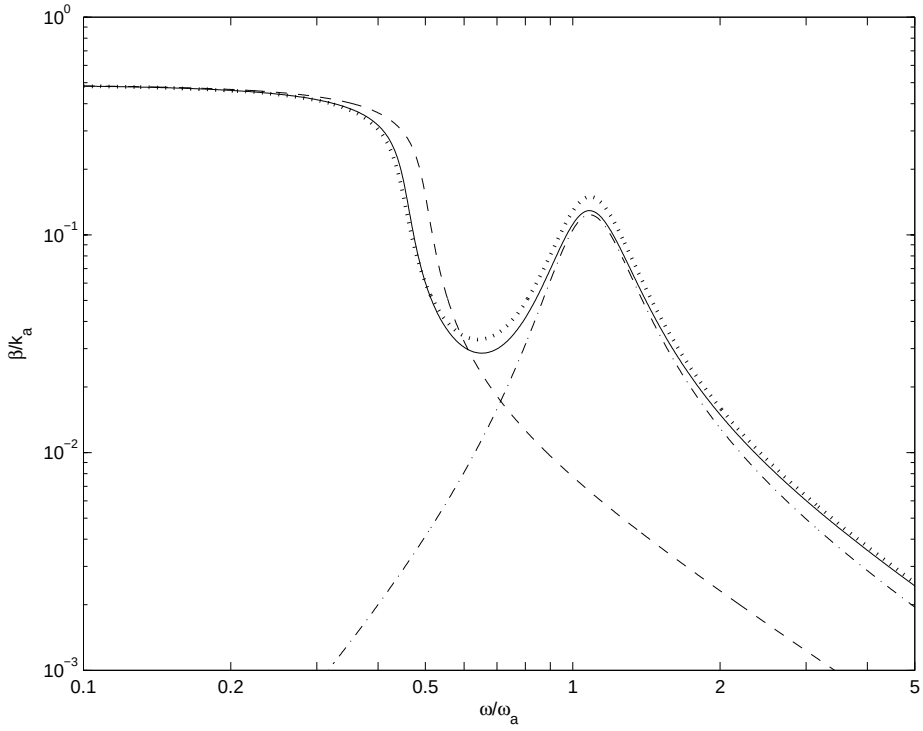

Figure 15. Normalised decay rate of supported Euler-Bernoulli beam with tuned absorbers, $\mu = 0.2$, $\omega_0 = 0.5\omega_a$, $\eta = 0.1$, $\eta_a = 0.4$. ·····, direct calculation of supported beam with absorber; – · – ·, absorber on free beam; – – –, supported beam with no absorber; —, sum of decay rates of absorber on free beam and supported beam including absorber mass.

8. Two-layer foundation viewed as an absorber

In this section a beam on a two-layer foundation is considered, as shown in Figure 16. This can represent, for example, a railway track consisting of a rail supported on sleepers, with resilient rail pads between the rail and sleeper and ballast beneath the sleeper providing a further layer of resilience. It has long been recognised that the sleeper mass forms a dynamic absorber which increases the rail decay rate in a particular frequency band (Thompson and Vincent 1995). The analysis here shows the effect of including the absorber mass within the foundation in this way. The stiffness per unit length of the upper spring is denoted s_1, the mass per unit length of the intermediate mass is m_s' and s_2 is the stiffness per unit length of the lower spring.

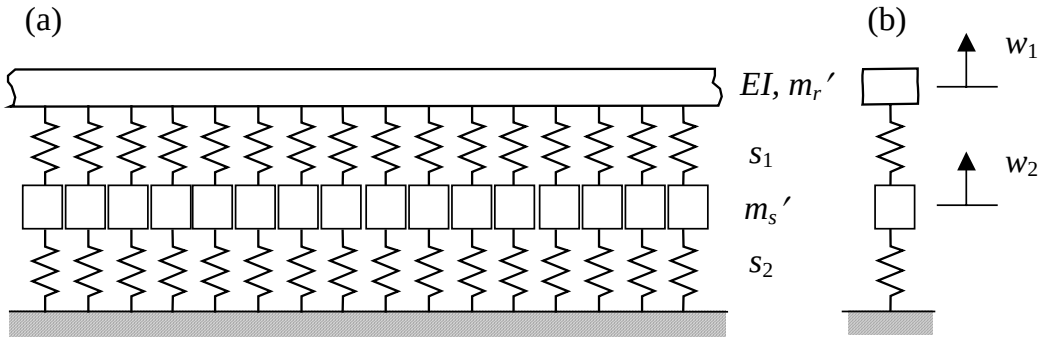

Figure 16. (a) Beam on two-layer foundation, (b) equivalent mass-spring system.

The analysis of Section 3 can be repeated but with a frequency-dependent support stiffness, $s(\omega)$, which in the undamped case is given by

$$s(\omega) = \frac{s_1(s_2 - \omega^2 m_s')}{(s_1 + s_2 - \omega^2 m_s')} \tag{48}$$

Damping can be added as before by making s_1 and s_2 complex with loss factors η_1 and η_2 respectively. If the beam is constrained, the mass m_s' vibrates freely on the combined stiffness of the two layers at the frequency ω_a, given by

$$\omega_a = \sqrt{\frac{s_1 + s_2}{m_s'}} \tag{49}$$

This corresponds to an *anti*-resonance of the support as seen at the beam and is in effect the tuning frequency of the two layer support at which it acts as a neutraliser to the beam.

There are two frequencies at which $m_r'\omega^2 - s(\omega) = 0$, corresponding to the condition of cut-off seen in Section 3. These cut-off frequencies are the natural frequencies of the corresponding two-degree-of-freedom system shown in Figure 16(b). From the equations of motion of the two-degree-of-freedom system, these frequencies can be found as

$$\omega_c^{\,2} = \frac{(\omega_1^{\,2} + \omega_a^{\,2})}{2} \pm \sqrt{\frac{(\omega_1^{\,2} + \omega_a^{\,2})^2}{4} - \omega_1^{\,2}\omega_2^{\,2}} \tag{50}$$

where ω_1 and ω_2 are given by

$$\omega_1 = \sqrt{\frac{s_1}{m_r'}},\ \omega_2 = \sqrt{\frac{s_2}{m_s'}} \tag{51a,b}$$

The two cut-off frequencies ω_c are plotted in Figure 17 for different values of $\mu = m_s'/m_b'$ and $\kappa = s_1/s_2$. These results have been normalised by the absorber tuning frequency ω_a from

Eq. (45). The absorber bandwidth [ω_a, ω_{c2}] can be seen to be smaller than the corresponding result from Eq. (15), shown by the circles, which forms the limit as $s_2 \to 0$.

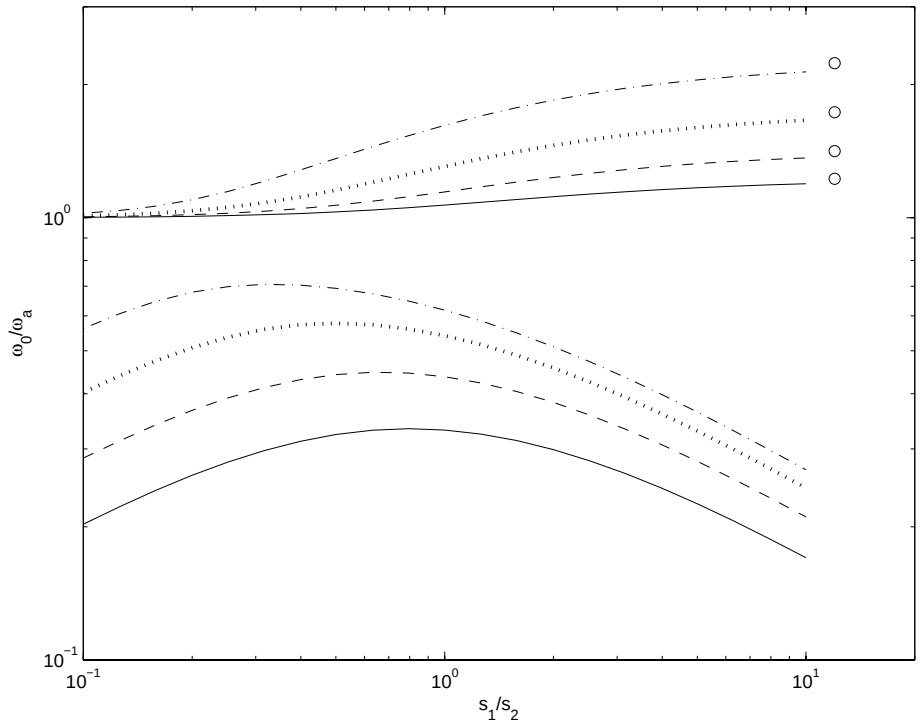

Figure 17. Bounding frequencies of propagating wave behaviour shown relative to 'absorber tuning frequency' of two-layer foundation. —, $\mu = 0.5$; – – –, $\mu = 1$; ·····, $\mu = 2$; – · – · –, $\mu = 4$; o, limit for $s_2 = 0$.

Examples of the wavenumbers are shown in Figure 18. These are shown normalised to the free beam wavenumber at ω_a. These results are given for $\mu = 4$, which is typical of a railway track with concrete sleepers, although much larger than considered in earlier sections.

As for the case of a single stiffness support, below the cut-off frequency ω_{c1}, a low frequency 'blocked' region occurs where no waves propagate, the wavenumbers having equal real and imaginary parts. Free wave propagation occurs in the whole of the region between ω_{c1} and ω_a. At ω_a the support stiffness $s(\omega)$ becomes infinite and changes sign and free wave propagation ceases. There follows a second 'blocked' region of complex wavenumbers between ω_a and ω_{c2}, in which the wavenumber falls with increasing frequency, above which free wave propagation again commences. At high frequency the wavenumber tends to that of the

unsupported beam, k_b. The region between ω_a and ω_{c2} resembles that of the absorber seen in Section 4.

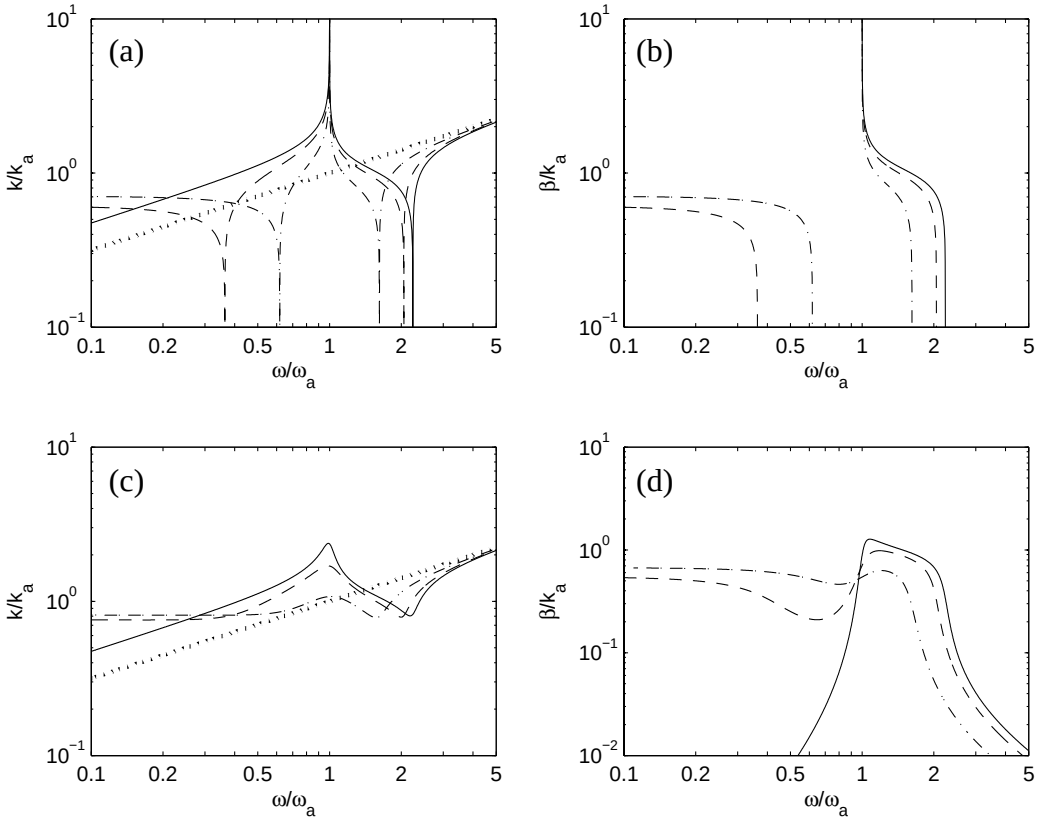

Figure 18. First wavenumber for beam on two-layer foundation, $\mu = 4$. —, $\kappa = \infty$ ($s_b = 0$); – – –, $\kappa = 5$; – · – · $\kappa = 1$, ····· free beam. Frequency normalised by ω_a, wavenumbers by beam free wavenumber at ω_a. (a) Real part of first wave, undamped, (b) imaginary part of first wave, undamped, (c) real part of first wave, $\eta_1 = 0.1$, $\eta_2 = 1$, (d) imaginary part of first wave, $\eta_1 = 0.1$, $\eta_2 = 1$.

As the stiffness of the lower layer (s_2) increases, relative to s_1, the width of the blocked zone above ω_a reduces, making the absorber less effective. Conversely, the blocked region at low frequency extends higher in frequency.

Also shown in Figure 18 are results including damping in the support layers. These show similar trends to the undamped results, with the 'blocked' regions still discernible below ω_{c1} and between ω_a and ω_{c2}. The attenuation (imaginary part) is no longer zero outside these blocked regions. As for the undamped case, the effectiveness of the intermediate mass acting

as an absorber can be seen to reduce as the stiffness of the lower layer increases. For smaller values of μ, not shown, the bandwidth of the absorber peak is reduced and again it is further reduced as κ reduces.

Clearly, significant attenuation can be introduced to the beam over a frequency bandwidth of at least an octave by a configuration with a mass ratio $\mu = 4$ and stiffness ratio $\kappa = 5$. These values are quite typical of a railway track with concrete sleepers (Thompson and Vincent 1995). Thus it is confirmed that the sleeper in a railway track acts like a tuned absorber. Since it has quite large mass compared with the beam, large attenuation is possible over a wide frequency range. The effectiveness is reduced, however, as the stiffness of the upper resilient layer is reduced relative to that of the lower layer.

9. Results for other wave types

9.1 Non-dispersive waves

The results throughout this report have been for waves in an Euler-Bernoulli beam. In this section the case of a system carrying non-dispersive waves is considered briefly as an alternative. These may be longitudinal or torsional waves of a rod or shear waves. The latter can be considered as a high frequency approximation to bending in a thick beam.

Taking as an example the longitudinal motion of a beam on an elastic foundation, the equation of free vibration for harmonic motion at frequency ω is

$$EA\frac{d^2u}{dx^2} - \left(s - m_b'\omega^2\right)w = 0 \tag{52}$$

where u is the complex vibration amplitude and x is the coordinate along the beam direction. This is a second order equation as opposed to the fourth order bending equation of Eq. (1). The wavenumber in the supported beam, $\tilde{k} = k - i\beta$ has solutions

$$\tilde{k} = \pm\sqrt{\frac{m_b'\omega^2 - s}{EA}} = \pm k_l\sqrt{1 - \frac{\omega_0^2}{\omega^2}} \tag{53}$$

where $\omega_0 = (s/m_b')^{1/2}$ is the resonance frequency of the beam mass on the support stiffness as before and $k_l = (\omega^2 m_b'/EA)^{1/2}$ is the wavenumber of the unsupported beam. In the absence of damping, the wavenumber $\tilde{k}$ has purely real solutions for frequencies above ω_0, while for frequencies below ω_0, it is purely imaginary. For $\omega << \omega_0$, the imaginary part

$\beta \approx k_0 = (s/EA)^{1/2}$, which is equal to the wavenumber of the unsupported beam, k_l, at frequency ω_0.

Introducing damping into the support and the beam itself by means of loss factors η and η_b, gives complex wavenumbers

$$\tilde{k} = k_l(1+i\eta_b)^{-1/2}\left(1-\left(\frac{\omega_0}{\omega}\right)^2(1+i\eta)\right)^{1/2} \tag{54}$$

Note that these have terms to the power ½ where the bending equation, Eq. (6), had terms to the power ¼. At high frequency, for $\omega >> \omega_0$, the imaginary part is given by

$$\beta \approx k_l\left(\frac{\eta_b}{2}+\frac{\eta}{2}\left(\frac{\omega_0}{\omega}\right)^2\right). \tag{55}$$

which differs from Eq. (7) by a factor of 2 as well as the presence of the wavenumber for longitudinal waves k_l.

Introducing an absorber for longitudinal motion to a free beam, the frequency-dependent stiffness corresponding to the absorber is identical to Eq. (9). The wavenumber in the beam in the presence of the mass-spring system is modified to

$$\tilde{k}^2 = k_l^2\left(1+\mu\frac{1+i\eta_a}{1+i\eta_a-(\omega^2/\omega_0^2)}\right) \tag{56}$$

The bandwidth of the blocked region for the undamped case is identical to that for bending, Eq. (15), but in this region the wavenumber is now purely imaginary.

For the damped absorber, the imaginary part of the wavenumber far above the tuning frequency is given by

$$\beta \approx \frac{k_l}{2}\frac{\omega_a^{\,2}}{\omega^2}\mu\eta_a \quad \text{for } \omega >> \omega_a \tag{57}$$

while at low frequencies

$$\beta \approx \frac{k_l}{2}\frac{\omega^2}{\omega_a^{\,2}}\mu\eta_a \quad \text{for } \omega << \omega_a \tag{58}$$

Comparing these with Eqs (21) and (23), they again differ by a factor of 2 as well as the modified wavenumber.

Evaluating the wavenumber at ω_b, which is at the centre of the blocked zone for the undamped case, gives

$$\beta = -k_l \,\mathrm{Im}\left\{\left(1-\frac{\mu(1+i\eta_a)}{\mu/2-i\eta_a}\right)^{1/2}\right\} \text{ for } \omega = \omega_b \tag{59}$$

As before, two extreme cases can be considered. Firstly, for small damping $\eta_a << \mu/2$ (and $\eta_a << 1$) the decay rate is independent of both the mass ratio and the loss factor,

$$\beta = k_l \tag{60}$$

Secondly, for large damping $\eta_a >> \mu/2$ (and $\mu << 2$), Eq. (59) reduces to

$$\beta = \frac{k_l}{2}\frac{\mu}{\eta_a} \tag{61}$$

Thus for non-dispersive waves, similar results are found to those for bending waves, but in each case the attenuation is greater by a factor of 2 (a factor of $\sqrt{2}$ in the blocked zone for the lightly damped case) and is proportional to k_l, which is in turn proportional to ω rather than $\omega^{1/2}$. Thus greater attenuation can be expected at high frequency and a reduced effect below the tuning frequency.

9.2 Timoshenko beam

At high frequencies beams no longer behave according to the Euler-Bernoulli equations. Timoshenko beam theory offers an improvement by including shear deformation and rotational inertia, leading to an increase in the wavenumber. For the vertical bending of a rail this correction is found to be necessary above about 500 Hz, which is also typically where free waves commence (Thompson and Vincent 1995).

The wavenumbers corresponding to a UIC60 rail (see Thompson and Vincent 1995) normalised to an absorber tuning frequency of 1 kHz are shown in Figure 19. From this it can be seen that the wavenumber of the Timoshenko beam tends to that of a shear wave at high frequencies, $k = \omega\sqrt{m_b'/GA_s}$ where G is the shear modulus and A_s the reduced cross-section area effective in shear. For the particular choice of parameters, the shear wavenumber and the Euler-Bernoulli bending wavenumber cross at $2\omega_a$. Thus it can be expected that the results at frequencies well above ω_a will follow the trends described in Section 9.1.

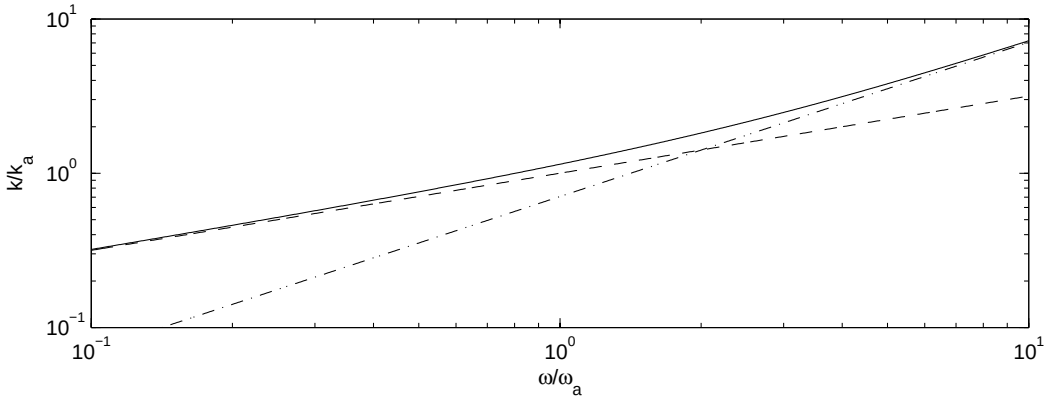

Figure 19. Normalised wavenumbers. — Timoshenko beam tuned absorbers, $\eta_a = 0.4$, $\mu = 0.2$; – – –, Euler-Bernoulli beam, – · – ·, shear beam.

In Figure 20 the decay rates are shown for a Timoshenko beam with added continuous absorber in comparison with an Euler-Bernoulli beam, all other parameters remaining as before. Higher decay rates are obtained at high frequencies using the Timoshenko beam. This can be attributed to the change in wavenumber.

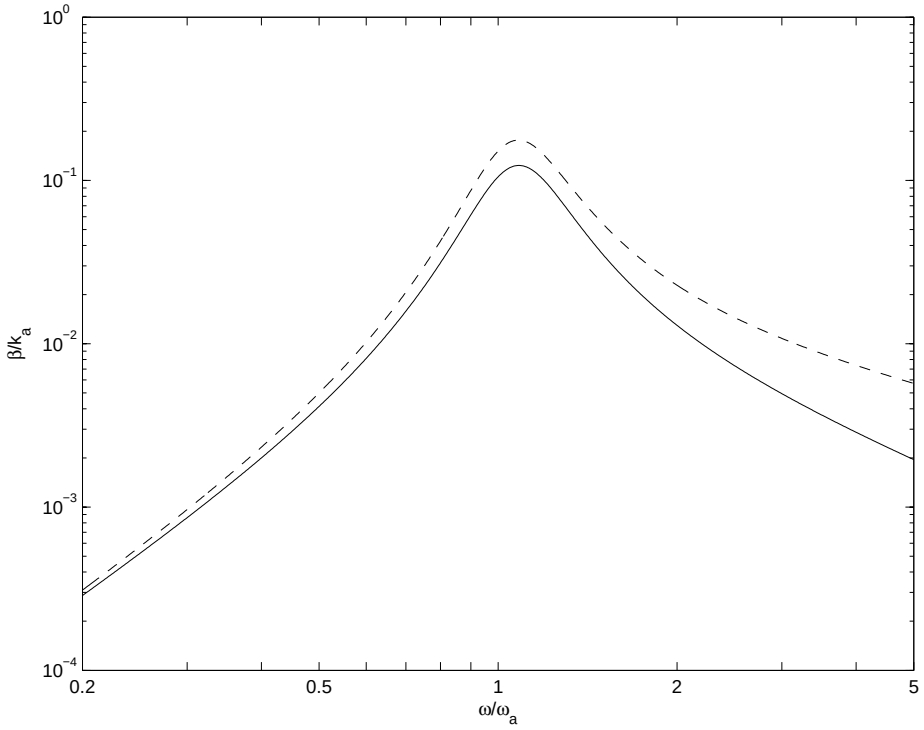

Figure 20. Normalised decay rate of beam with tuned absorbers, $\eta_a = 0.4$, $\mu = 0.2$. – – –, Timoshenko beam; —, Euler-Bernoulli beam.

Figure 21 shows the ratio of decay rates and the ratio of free wavenumber in each case. In the various expressions for the decay rate, Eqs (21), (23) and (30), the factor $k_b/4$ is present. Changing from an Euler-Bernoulli beam to a Timoshenko beam increases k_b as seen here and also changes the factor 4 in the above equations to a factor of 2 as seen in the previous subsection for longitudinal waves.

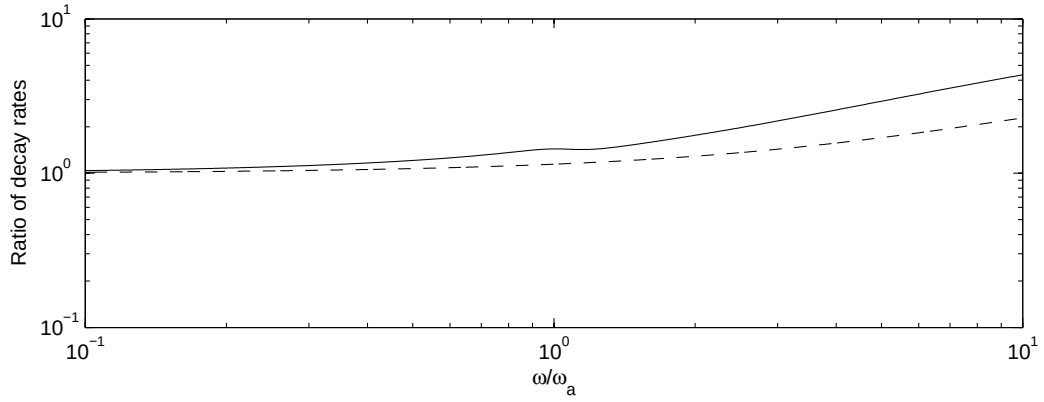

Figure 21. Effect of changing from Timoshenko beam to Euler-Bernoulli beam. — Ratio of decay rates with tuned absorbers, $\eta_a = 0.4$, $\mu = 0.2$; – – –, ratio of free wavenumbers.

From this discussion it can be expected that similar phenomena will be observed for a Timoshenko beam as were seen above for an Euler-Bernoulli beam, but that the performance of the absorber will be improved at high frequencies, which will improve both the peak decay rate and the frequency bandwidth.

10. Practical application to railway track

Various configurations of absorber applied to railway track are described in (Thompson & Gautier 2007). One particular application, described in (Thompson *et al.* 2007), has a total mass per unit length of 17.5 kg/m. For rails with mass per unit length 60 kg/m this corresponds to a mass ratio μ of 0.3. It has two steel masses on each side of the rail, separated from each other and from the rail by layers of an elastomeric material. This gives two resonances in the vertical direction in a suitable ratio (about a factor of 2 apart), which is effective in reducing the vertical bending motion of the rail; this was the dominant noise source for the track considered. A three-frequency system was also considered but found to give negligible additional benefit in terms of the overall noise. For the lateral direction it was

not possible to obtain two natural frequencies in a suitable ratio within the geometric constraints but this is of less importance for the overall noise.

The actual design was developed using finite element models of the rail and absorber cross-section. This allows for the cross-sectional deformation that occurs in the rail at higher frequencies (Thompson 1993). Extensive tests were also carried out on material samples to arrive at a suitable elastomer. In order to meet the requirement for a high loss factor, the elastomer operates in its transition region and there is therefore a high dependence of both stiffness and damping with temperature and frequency.

Field measurements on a track fitted with a prototype rail absorber were conducted as part of the 'Silent Track' EU project (Hemsworth *et al.* 2000, Thompson & Gautier 2007). The decay rates in the track were measured using impact excitation and rolling noise measurements were made using a test train.

Measurements showed an overall noise reduction of 5.6 dB(A). In order to show the reduction in track noise most clearly, these results were for a low-noise wheel (Hemsworth *et al.* 2000). Estimates in which the wheel noise is removed indicate that the track noise was reduced by about 6 dB(A) due to the absorber in this situation, although this will depend on the track design, in particular the stiffness of the rail pad. Further details are given in (Thompson *et al.* 2007).

11. Conclusions

The use of a continuous, damped mass-spring system added to a beam has been shown to be effective in increasing the attenuation of propagating structural waves in the beam and hence reducing the radiated noise. It is effective at any tuning frequency, independent of the bending wavelength in the beam, and so is particularly useful for stiff beams or at low frequencies, where constrained layer damping would be impractical. This has been developed for the particular application to a railway track but could also be considered for piping systems and many other beam-like structures.

Approximate formulae for the effect have been derived. The effective frequency bandwidth increases as the mass of the absorber is increased. Although the bandwidth is independent of

the absorber damping loss factor for low damping, for moderate damping the bandwidth increases as the damping is increased. For large values of loss factor the height of the decay rate peak is reduced. For a given mass, the effective bandwidth can also be increased by dividing the mass to form multiple absorbers with different tuning frequencies, although the height of the decay rate peak is reduced as a result. A practical application with two tuning frequencies has been demonstrated in railway track yielding a 6 dB reduction in rolling noise.

For a beam on an elastic foundation, the addition of an absorber can be represented well by adding the decay rates of the unsupported beam with absorber and the supported beam without absorber but including the absorber mass. For a Timoshenko beam the increase in wavenumber due to shear deformation causes the absorber to be more effective than for the corresponding Euler-Bernoulli beam at high frequencies.

For a railway track with concrete sleepers, the mass of the sleeper acts as a tuned absorber which increases the decay rate over a wide frequency region. The large mass relative to the rail makes this an effective system. However, the fact that the absorber is integral to the support system in this case means that the benefit is less than that for a separate absorber of the same mass, especially if the rail pad is not much stiffer than the ballast layer below the sleeper.

References

Brennan, M.J. 1997a Vibration control using a tunable vibration neutralizer. Proc. Instn Mech. Engrs, Part C, 211C, 91-108.

Brennan, M.J. 1997b Characteristics of a wideband vibration neutralizer, Noise Control Engineering Journal 45, 201-207.

Brennan, M.J. 1998 Control of flexural waves on a beam using a tunable vibration neutraliser. J. Sound Vib. 222, 389-407.

Brennan, M.J. & Ferguson, N.S. 2004 Vibration control, chapter 12 in F. Fahy and J. Walker (eds) Advanced applications of acoustics, noise and vibration, London: E&FN Spon.

Clark, P. 1995 Devices for the reduction of pipeline vibration, PhD thesis, University of Southampton.

Cremer, L., Heckl, M. & Ungar, E.E. 1988 Structure-borne sound, Berlin: Springer, second edition.

De Jong, C.A.F. 1994 Analysis of pulsations and vibrations in fluid-filled pipe systems, PhD thesis, TNO Institute of Applied Physics, Delft.

Den Hartog, J.P. 1985 Mechanical Vibrations, New York: Dover Publications.

Estève, S.J. & Johnson, M.E. 2002 Reduction of sound transmission into a circular cylindrical shell using distributed vibration absorbers and Helmholtz resonators. J. Acoust. Soc. Am. 112(6), 2840-2848.

Fahy, F.J. 1985 Sound and structural vibration, London: Academic Press.

Fuller, C.R., Maillard, J.P., Mercadal, M. & von Flowtow, A.H. 1997 Control of aircraft interior noise using globally detuned vibration absorbers. J. Sound Vib. 203, 745-761.

Graff, K.F. 1991 Wave motion in elastic solids, New York: Dover Publications.

Hemsworth, B., Gautier, P.E. & Jones, R. 2000 Silent Freight and Silent Track projects. *Proceedings Internoise 2000*, Nice, France, 714-719.

Hunt, J.B. 1979 Dynamic Vibration Absorbers. London: Mechanical Engineering Publications.

Hunt, J.B. & Nissen, J-C 1982 The broadband dynamic vibration absorber, J. Sound Vib. 83, 573-578.

Jones, C.J.C., Thompson, D.J. & Diehl, R.J. 2006 The use of decay rates to analyse the performance of railway track in rolling noise generation. J. Sound Vib. 293, 485-495.

Maidanik, G. & Becker, K.J. 1999 Characterization of multiple-sprung masses for wideband noise control. J. Acoust. Soc. Am. 106, 3109-3118.

Marcotte, P., Fuller, C.R. & Cambou, P. 1999 Control of the noise radiated by a plate using a distributed active vibration absorber (DAVA), Proceedings of Active 99, Ft Lauderdale, FL, USA, 447-456.

Maurini, C., dell'Isola, F. & Del Vescovo, D. 2004 Comparison of piezoelectronic networks acting as distributed vibration absorbers. Mechanical Systems and Signal Processing 18, 1243-1271.

Mead, D.J. 2000 Passive vibration control, Chichester: John Wiley & Sons.

Nashif, A.D., Jones, D.I.G. & Henderson, J.P. 1985Vibration Damping, New York: John Wiley and Sons.

Newland, D.E. 2003 Vibration of the London Millennium Bridge: cause and cure, International Journal of Acoustics and Vibration 8, 9-14.

Newland, D.E. 2004 Pedestrian excitation of bridges, Proc. Instn Mech. Engrs, Part C, 218C, 477-492.

Ormondroyd J. & den Hartog, J.P. 1928 The theory of the dynamic vibration absorber, Transactions of the American Society of Mechanical Engineers, 50, A9-A22.

Rana, R. & Soong, T.T. 1998 Parametric study and simplified design of tuned mass dampers. Engineering Structures 20, 193-204.

Smith, T.L., Rao, K. & Dyer, I. 1986 Attenuation of plate flexural waves by a layer of dynamic absorbers, Noise Control Engineering Journal 26, 56-60.

Strasberg, M. & Feit, D. 1996 Vibration damping of large structures induced by attached small resonant structures. J. Acoust. Soc. Am. 99, 335-344.

Thompson, D.J. 1993 Wheel-rail noise generation part III: rail vibration. J. Sound Vib. 161, 421-446.

Thompson, D.J. & Vincent, N. 1995 Track dynamic behaviour at high frequencies. Part 1: theoretical models and laboratory measurements. Vehicle System Dynamics Supplement, 24, 86-99.

Thompson, D.J., Jones, C.J.C. & Turner, N. 2003 Investigation into the validity of two-dimensional models for sound radiation from waves in rails. J. Acoust. Soc. Am. 113, 1965-1974.

Thompson, D.J. & Gautier, P-E. 2007 A review of research into wheel/rail rolling noise reduction, Proc. Instn Mech. Engrs, Part F, *accepted for publication*.

Thompson, D.J., Jones, C.J.C., Waters, T.P. & Farrington, D. 2007 A tuned damping device for reducing noise from railway track. Applied Acoustics, 68, 43-57.

Zapfe, J.A. & Lesieutre, G.A. 1997 Broadband vibration damping using highly distributed tuned mass absorbers, AIAA Journal 35, 753-755.

Zivanovic, S., Pavic, A. & Reynolds, P. 2005 Vibration serviceability of footbridges under human-induced excitation: a literature review, J. Sound Vib. 279, 1-74.

Appendix A. Relation between radiated sound from an infinite beam and spatial attenuation rate

The general expression for the radiated sound power W_{rad} from a vibrating structure can be written as (Fahy 1985)

$$W_{rad} = \tfrac{1}{2}\rho_0 c_0 \sigma S \left\langle |v|^2 \right\rangle \tag{A1}$$

where S is the surface area, $\rho_0 c_0$ is the characteristic acoustic impedance of air, σ is the radiation ratio which depends on frequency and $\left\langle |v|^2 \right\rangle$ is the spatially averaged velocity amplitude normal to the surface. For an infinitely long beam along the x axis this can be expressed as

$$W_{rad} = \tfrac{1}{2}\rho_0 c_0 \sigma L \int_{-\infty}^{\infty} |v(x)|^2 \, dx \tag{A2}$$

where L is a perimeter length of the cross-section, $v(x)$ is the velocity amplitude at longitudinal position x. Above the cut-off frequency the evanescent wave component has only a small effect on the integral since it decays rapidly, and the above expression can be approximated by

$$W_{rad} \approx \tfrac{1}{2}\rho_0 c_0 \sigma L |v(0)|^2 \int_0^{\infty} \left| e^{-i\tilde{k}x} \right|^2 dx \tag{A3}$$

For a complex valued wavenumber $\tilde{k} = k - i\beta$, the integral reduces to

$$\int_0^{\infty} \left| e^{-i\tilde{k}x} \right|^2 dx = \int_0^{\infty} e^{-2\beta x} dx = \frac{1}{2\beta} \tag{A4}$$

giving

$$W_{rad} \approx \frac{\rho_0 c_0 \sigma L |v(0)|^2}{4\beta} \tag{A5}$$

which shows that the radiated power is inversely proportional to β and to the decay rate, $\Delta = 8.686\beta$.